U.PORTO

FEUP FACULDADE DE ENGENHARIA
UNIVERSIDADE DO PORTO

Alzheimer's disease: development of an immunosensor for amyloid beta detection

Pedro Jorge da Silva Carneiro

Supervisor: Prof. Dr. Maria do Carmo Silva Pereira

Co-Supervisor: Prof. Dr. Simone Barreira Morais

Master's Program in Biomedical Engineering

July, 2013

Abstract

Alzheimer's disease (AD) is a neurodegenerative pathology that becomes increasingly common with aging, characterized by extracellular accumulation of senile plaques (Aβ), intracellular appearance of neurofibrillary tangles and neuronal loss.

AD affects about 35 million people worldwide, and if current trends continue with no medical advancement, one in 85 people will be affected by 2050. Thus, there is an urgent need to develop a cost-effective, easy to use sensor platform to facilitate the diagnostic process, identify patients at an earlier stage and allow monitorization of biochemical effects of the treatments.

Since the quantification of amyloid beta (Aβ) has been established as a reliable test to diagnose AD through human clinical trials, an electrochemical immunosensor was designed and developed for detection of this biomarker in biological fluids and is the focus of this work. It is based on a gold electrode modified with mercaptopropionic acid self-assembled monolayer, electrodeposited gold nanoparticles and Aβ antibody. Antibodies act as the biorecognition element of the sensor and selectively capture and bind Aβ42 to the electrode surface. The antibodies were immobilized on gold nanoparticles that offered excellent properties for electroanalytical assays. Cyclic and square-wave voltammetry, as well as electrochemical impedance spectroscopy were used to characterize the construction of the biosensor. The optimum values for the relevant experimental variables were determined.

Using the proposed immunosensor, Aβ42 can be specifically detected within a range of 0.451–9028 ng/mL with a 264 pg/mL detection limit. The immunosensor enables real-time, rapid and highly sensitive detection of Aβ with low-cost and opens up the possibilities for diagnostic *ex vivo* applications and research-based *in vivo* studies.

Keywords: Alzheimer's disease, amyloid beta, electrochemical immunosensor, self-assembled monolayers, gold nanoparticles.

Acknowledgements

First and foremost, I would like to give my most sincere appreciation to my supervisors, Prof. Maria do Carmo Silva Pereira and Prof. Simone Barreira Morais for their continued support and guidance throughout my research project and in helping me develop scientific thinking and research knowledge.

Moreover I would like to give my thanks to Thiago Mielle from REQUIMTE for his essential support and assistance in the laboratory, Sílvia Coelho and Joana Loureiro from LEPAE for their help in the gold nanoparticles synthesis and antibody treatment, respectively. I am also grateful to all REQUIMTE and LEPAE team for their assistance and great work environment.

Finally I would like to give thanks to my parents, girlfriend and friends for their continued support and encouragement throughout this year.

List of Publications

Most of the content presented in this thesis was submitted or accepted for publication in:

1. Carneiro, P., Delerue-Matos, C., Morais, S., Pereira, M, Electrochemical Immunosensor for Amyloid Beta-Peptide Detection: Preliminary Study, 3rd Portuguese Bioengineering Meeting - Bioengineering National Congress, Braga February 2013.
2. Carneiro, P., Delerue-Matos, C., Morais, S., Pereira, M, Alzheimer disease: development of an immunosensor for biomarker detection, 6º Encontro de Investigação Jovem da Universidade do Porto, Porto February 2013.

Contents

List of Figures

List of Abbreviations

ABTS - 2,2′-Azino-bis(3-ethylbenzothiazoline-6-sulfonic acid) diammonium salt

Ab_2 – Secondary antibody

AC – Alternate current

AD – Alzheimer's disease

AFM – Atomic force microscopy

AICD – APP intracellular domain

AMPA - α-amino-3-hydroxy-5-methyl-4-isoxazolepropionic acid receptor

Anti-Aβ42 – Antibody against Aβ42

apoE - Apolipoprotein E

APOE34 – Apolipoprotein E34

APOJ – Apolipoprotein J

APP – Amyloid precursor protein

AuE – Gold electrode

AuNPs – Gold nanoparticles

Aβ – Amyloid beta peptide

BACE - Beta-site APP-cleaving enzyme

BSA – Bovine serum albumin

C_d – Double layer capacitor

CNS – Central nervous system

CR1 – Complement receptor 1

CSF – Cerebrospinal fluid

CV – Cyclic voltammetry

CYS - Cystamine

CYS+ME – Cystamine + Mercaptoethanol

C99 – 99 amino acid C-terminal fragment of APP

DNA – Deoxyribonucleic acid

EDC - N-(3, Dimethylaminopropyl)-N-ethyl-carbodiimide hydrochloride

EDTA - Ethylenediaminetetraacetic acid

EIS – Electrochemical impedance spectroscopy

ELISA – Enzyme-linked immunosorbent assay

FDG - Fluorodeoxyglucose

GPES – General Purpose Electrochemical system for Windows software

HPLC – High-performance liquid chromatography

Ig - Immunoglobolin

IHP - Inner Helmholtz plane

LOD – Detection limit

LOQ – Quantification limit

LTD – Long-term depression

LTP – Long-term potentiation

MPA – Mercaptopropionic acid

MPA+ME – Mercaptopropionic acid + Mercaptoethanol

MRI – Magnetic resonance imaging

MTA – Medial temporal atrophy

NHS - N-hydroxysuccinimide

NMDA - N-methyl-D-aspartic acid

NSB – Nonspecific binding

OHP - Outer Helmholtz plane

PBS - Phosphate buffer saline

PEG - Polyethylene glycol

PET – Positron emission tomography

PICALM - Phosphatidylinositol binding clathrin assembly protein

PS1 – Presenilin 1

PS2 – Presenilin 2

R_{ct} – Charge transfer resistance

R_p – Polarization resistance

R_s – Solution resistance

SAM – Self-assembled monolayer

SEM – Scanning electron microscopy

SORL1 - Sortilin-related receptor, L(DLR class) A repeats containing

STM – Scanning tunneling microscopy

SWV – Square-wave voltammetry

TEM – Transmission electron microscopy

TOMM40 - Translocase of outer mitochondrial membrane 40 homolog

Zw – Warburg impedance

β-CTF – β-C-terminal fragment

1. Introduction

Alzheimer's disease (AD) is the most common form of dementia in the elderly [1, 2]. AD is a neurodegenerative disorder that causes global, progressive and irreversible deterioration of many cognitive functions as memory, concentration, speaking capability, thought and eventually causes death. This deterioration leads to changes in behavior, personality and functional capacity, which hampers the daily life of the patient. As the population ages, AD is rapidly becoming an urgent public health problem. Nowadays, it affects 35 million individuals worldwide and it is projected to affect 115 million by 2050 [3]. In Portugal this number is estimated to be 90 000 [2]. Without the prevention and development of new therapies for AD, both health care and socioeconomic systems will not be able to support the financial needs of AD in the future [4].

Pathological hallmarks of AD include extracellular deposits of amyloid β peptides (Aβ) (senile plaques), intraneuronal inclusions of hyperphosphorylated tau protein in neurofibrillary tangles, together with downstream processes such as inflammation and oxidative stress, all of which contribute to loss of synaptic integrity, effective neural network connectivity and progressive neurodegeneration [3-5].

Research gives support to the "amyloid cascade hypothesis", which advocates that an imbalance between the production and clearance or degradation of Aβ in the brain is the initiating event in AD, leading to synaptic and neuronal dysfunction and degradation resulting, consequently, in cognitive disturbances [6].

The current diagnostic procedures of AD are difficult and are made in an advanced stage of the disease [4]. Therefore it is clinically important to find accurate markers for AD by new non-invasive methods that may facilitate the diagnostic process, identify patients at an earlier stage and monitor biochemical effects of the treatments [4].

There is a continuing demand for fast and simple analytical methods for the determination of many clinical and biochemical parameters. The requirement for immunologically based biosensors is generally considered to be in the diagnostic field and particularly in the home diagnostic field. Immunoassays and immunosensors rely on the antibody-antigen interactions providing promising means of analysis due to their specificity and sensitivity. The high specificity is achieved mainly by the molecular recognition of the target analytes by the antibodies or antigens forming stable

immunocomplexes [7-9]. On the other hand, sensitivity depends on several factors, including the affinity of antibodies, the amount of immobilized immunological recognition elements, and the choice of transducer and signal probe [8]. The improvement of immunoassay and immunosensor performance mainly relies on the development of antibody preparation techniques, the improvement of immobilization and tagging methods, and the adoption of a high-performance transduction method [8]. Electrochemical detection overcomes problems associated with other immunoassays and immunosensors detection techniques, such as the short half-life of radioactive agents and concerns of health hazards, while limited sensitivity in the analysis of colored or turbid samples is achieved in immunoassays coupled with optical detection [10].

Electrochemistry is the science concerned with the physical and chemical properties of ionic conductors as well as with phenomena occurring at the interfaces between ionic conductors and electronic conductors or semiconductors, or even insulators (including gases and vacuum) [11, 12]. In other words, electroanalytical methods are a class of techniques in analytical chemistry which studies the relationship between electrical and chemical parameters enabling the detection of the analyte of interest by measuring the potential and/or current in an electrochemical cell. Such electroanalytical measurements have been found to have a vast range of applications, including biomedical analysis, quality control, and environmental monitoring. Electrochemical transducers for immunoassays and immunosensors are very attractive due to their high sensitivity, inherent simplicity and miniaturization, low cost and power requirements [8, 9, 13]. Furthermore, electrochemistry is an interfacial process in which the relevant reactions take place at the electrode-solution interface, rather than in bulk solution [12]. Therefore, in conjunction with developments in micro- and nano-electrochemical sensors, electrochemistry offers an added bonus of detecting analytes in very small volumes [8, 10].

1.1 Main Objectives

The aim of this research is to develop a sensitive gold label free immunosensor for the Alzheimer's disease main biomarker, amyloid-beta peptide, in order to facilitate and enable early AD diagnosis. The immunosensor construction comprises three main steps:

1. Formation of a self-assembled monolayer on the gold surface in order to control the electrode interface. Several self-assembled monolayers (SAMs) were tested and experimental conditions were optimized in order to promote the best immobilization on the gold surface.
2. Electrodeposition of gold nanoparticles on the modified SAM/gold electrode. Gold nanoparticles enhanced the biosensor response and allowed antibody immobilization. Different methods for gold nanoparticles synthesis were tested and compared.
3. Immobilization of the antibody on the gold nanoparticles/SAM/gold electrode. Concentration of the antibody and time of incubation were optimized in order to promote the desired immobilization.

   The electroanalytical behavior of the developed biosensor was characterized in terms of calibration data. Finally, it was successfully applied to synthetic solutions of Aβ.

1.2 Thesis structure

This thesis is divided in 6 chapters.

In Chapter 1, the key issues are introduced. The motivations to the work performed, as well as, the main objectives of the work are presented.

In Chapter 2 the theoretical aspects concerning the main topics of this work are presented. The following subjects are discussed: the formation of extracellular deposits of Aβ and consequently development of AD, the main electrochemical technique principles, the characteristics of biosensors and immunoassays, properties of nanomaterials and their importance in the development of biosensors. In this section the recent studies related with this theme are also referred.

Chapter 3 describes the reagents, equipments and methods used in the performed experiments.

In Chapter 4, the results attained are presented and discussed. The topics include the characterization of the gold electrode, the SAMs formation, synthesis and electrodeposition of gold nanoparticles, antibody immobilization and finally detection of Aβ.

Chapter 5 is the final chapter of the thesis in which the main conclusions and future perspectives for the work are referred.

2. State of the Art

2.1 Alzheimer's disease – The amyloid cascade hypothesis

AD is a neurodegenerative pathology characterized by extracellular deposits of Aβ peptide (senile plaques), intracellular appearance of neurofibrillary tangles and neuronal loss.

The amyloid cascade hypothesis defends that the deposition of the Aβ peptide in the brain parenchyma is a crucial step that ultimately leads to AD (Figure 1) [6, 14]. Autosomal dominant mutations that cause early onset familial AD occur in three genes: amyloid precursor protein (APP), presenilin 1 (PS1) and presenilin 2 (PS2*)* [6, 14]. The first genetic mutations causing AD were discovered in the APP gene [6]. Most of the mutations cluster at or very near the sites within APP that are normally cleaved by proteases called α-, β-, and γ- secretases [6]. These mutations promote generation of Aβ by favoring proteolytic processing of APP by β- or γ-secretase [4, 6, 14]. Besides the mutations in the PS1 and PS2 genes that alter the APP metabolism through a direct effect on the γ-secretase, four important observations were given to support the amyloid cascade hypothesis. Firstly, the deposition of tau protein in neurofibrillary tangles in the brain occurs without deposition of amyloid [6]. The conclusion is that even the most severe consequences of tau alteration namely, neurofibrillary tangle formation leading to neurodegeneration, are not sufficient to induce the amyloid plaques [6]. This way, the formation of neurofibrillary tangle of tau is likely to be deposited after changes in Aβ metabolism and initial plaque formation, rather than before [6]. Secondly, studies suggest that altered APP processing occurs before tau alterations in the cascade of AD, a notion bolstered by the observation that Aβ toxicity is tau dependent [6]. Thirdly, studies where APP transgenic mice were crossed with apolipoprotein E (apoE) deficient mice, cerebral Aβ deposition was reduced in the offspring, providing strong evidence that the pathogenic role of genetic variability at the human apoE locus is very likely to involve Aβ metabolism [6, 14]. At last, evidence indicates that genetic variability in Aβ catabolism and clearance may contribute to the risk of late-onset AD [6]. These four findings reinforce the theory that cerebral Aβ accumulation is the primary event in AD.

These studies have identified multiple steps potentially vulnerable to pharmacologic manipulation that resulted in the development of new drug candidates with disease-modifying potential [4]. This predicts a new type of causal mechanistic

treatment beyond symptomatic therapy [3, 4]. This new type of disease-modifying drugs is expected to be most effective if administrated very early in the disease process, before the neurodegenerative process is too severe [3, 4]. However, with the current techniques, the clinical diagnosis of AD can only be made when it is in an advanced stage. Thus, there is a great need for improved diagnostic tools and biomarkers appear as huge promise for the early identification of AD [3-5]. Biomarkers can provide a faster and more convenient responses to some questions and are playing increasingly diverse roles in drug development [3].

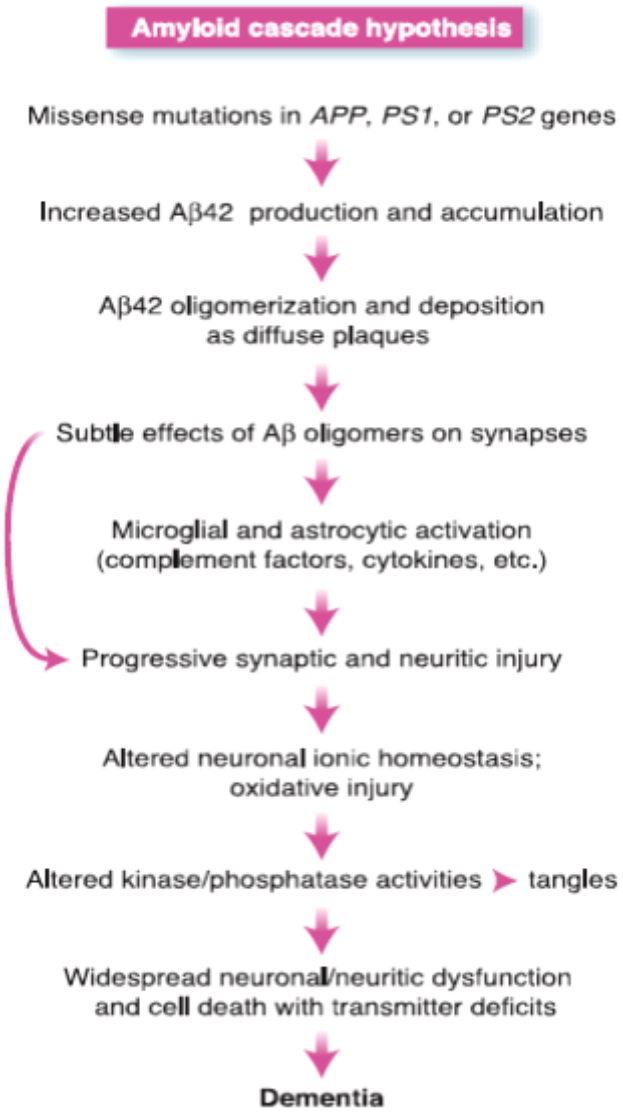

Figure 1 - The amyloid cascade hypothesis [6].

2.2 Biomarkers for Alzheimer's disease

"A biomarker (biological marker) is defined as a characteristic that is objectively measured and evaluated as an indicator of normal biological processes, pathogenic processes, or pharmacologic responses to a therapeutic intervention" [3]. In other words, the term biomarker is used to describe any neurochemical agent that is used to evaluate the risk or presence of disease. In this case, biomarkers may facilitate the ability to reliably diagnose AD in very early and perhaps even pre-clinical disease stages [4, 5]. They may also provide objective and reliable measures of drug safety and disease-modifying treatment efficacy in clinical drug trials in AD. Since the neuropathological changes and symptoms of AD take years to be noticed, the ideal therapy would be to treat the neuropathology as early as possible and biomarkers of pre-clinical AD are likely to play a fundamental role in the development of new therapies [4, 5]. Biomarkers can provide new insights into the neurobiology of AD and generate new and novel therapeutic targets. Disease-related biomarkers can assist in patient selection, sample stratification, course prediction and defining disease severity [3]. Biomarkers may assist in decision making in early clinical development, may inform corporate decisions regarding go or non-go decisions and may decrease cycle time and decrease costs [3].

The key features of an ideal AD biomarker are that it should detect a fundamental feature of the neuropathology, and have a diagnostic sensitivity for AD exceeding 80% together with specificity above 80% for distinguishing AD from other dementias [4]. It should also be reliable, reproducible, non-invasive, simple to perform, and inexpensive [3, 4]. The steps to establish a biomarker consist of confirmation by at least two independent studies conducted by qualified investigators with the results published in peer-reviewed journals, and validation in neuropathologically confirmed cases [4]. Beyond these criteria it would also be important if the biomarker could follow natural disease progression even as the effects of disease-modifying therapies [3-5].

Disease biomarkers may have important roles in three areas: as markers of trait, state, and rate [3, 15]. Trait markers represent risk factors and do not change with the presence of the disease [3, 15]. Trait biomarkers that are representative of an increased risk of AD include the apolipoprotein E 34 (APOE 34) allele [3, 16, 17], APOJ [3, 18, 19], CR1 [3, 19], PICALM [3, 18], SORL1 [3, 20], and TOMM40 [3]. State markers indicate the presence of the disease process and include medial temporal atrophy (MTA) on magnetic resonance imaging (MRI), amyloid imaging, and cerebrospinal fluid (CSF)

Aβ and tau protein measures [3]. Rate biomarkers follow disease progression; progressive atrophy detected by MRI and hypometabolism observed on fluorodeoxyglucose (FDG) positron emission tomography (PET) are rate biomarkers that correlate with disease severity [3].

Biomarkers can be collected from a variety of biological compartments (e.g., imaging of brain [3], cerebrospinal fluid Aβ and tau levels [3, 21]) and each compartment provides a different perspective on the pathological processes of AD (Figure 2) [3]. Imaging biomarkers provide insight into the topographic distribution of pathologic changes. Fluid biomarkers may appear in the central nervous system (CNS) compartments by diffusion and are subject to metabolism and excretion; the status of these mechanisms will also affect the relationship of the biomarker to the brain disease [3].

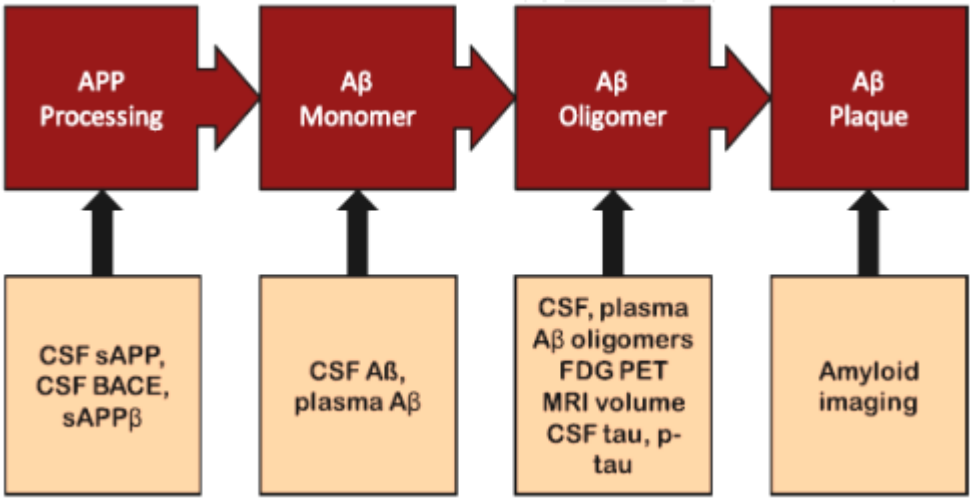

Figure 2 - Biomarkers for each step in the amyloid cascade [3].

The levels of Aβ42 in the CSF in AD are reduced due to deposition of the peptide in Aβ plaques in the brain and the levels of Aβ40 remain unchanged or may be moderately increased. Several studies have examined plasma levels of Aβ in AD but the findings were contradictory [3, 4]. Some groups reported high levels of Aβ40 and Aβ42 in plasma [4]. On the other hand other groups found no change in the Aβ plasma levels [4]. Tau protein levels in CSF increase during the development of AD [3]. Clusterin levels have been found to be increased in brain and CSF of patients with AD, and plasma clusterin was recently reported to be associated with brain atrophy, baseline disease severity, and rapid clinical progression in patients with AD [3]. In this study Aβ is the biomarker that will be explored.

2.2.1 Biological biomarkers of Aβ-related mechanism

As reported earlier, Aβ is generated by proteolytic cleavage (enzymatic digestion involving β- and γ-secretase activities [22]) of the type I transmembrane spanning glycoprotein amyloid precursor protein (APP) (Figure 3) [4, 5, 14, 22]. APP is cleaved at the N-terminus after position 671 by a protease referred to as β-secretase, also known as beta-site APP-cleaving enzyme (BACE) [4, 5, 14, 22]. This cleavage results in the release of a large N-terminal derivative called β-secretase-cleaved soluble APP (β-sAPP). At last, the 99 amino acid C-terminal fragment of APP (C99) is cleaved by the γ-secretase complex releasing free Aβ [4, 5, 14, 22].

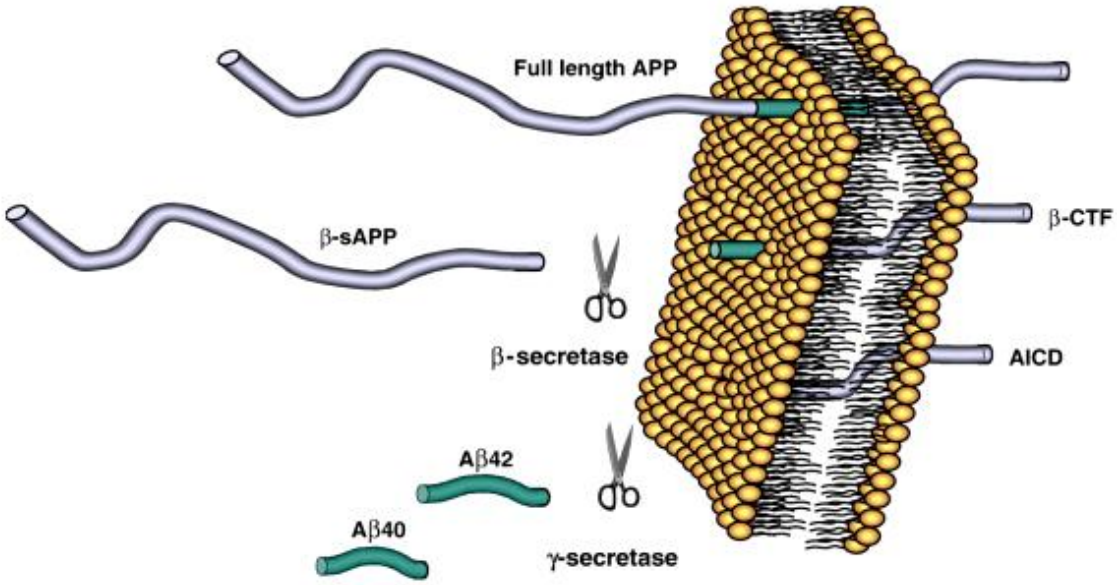

Figure 3 - Proteolytic cleavages of APP [4].

Once released, the Aβ peptide can be identified in cerebrospinal fluid and plasma, what makes the various species of Aβ really interesting as candidates to biomarkers [4]. The mechanism that enables Aβ monomers to aggregate is not well understood but Aβ can exist as monomers, dimmers, oligomers, protofibrils, fibrils and fibrillar aggregates (Figure 4) [3, 4]. Furthermore, the tendency of Aβ to aggregate seems to be related with the peptide's primary sequence as Aβ42 variant, which constitutes less than 10% of total Aβ, seems more prone to aggregate than more abundant Aβ40, contributing to the modification of the ratio Aβ40/Aβ42 [4].

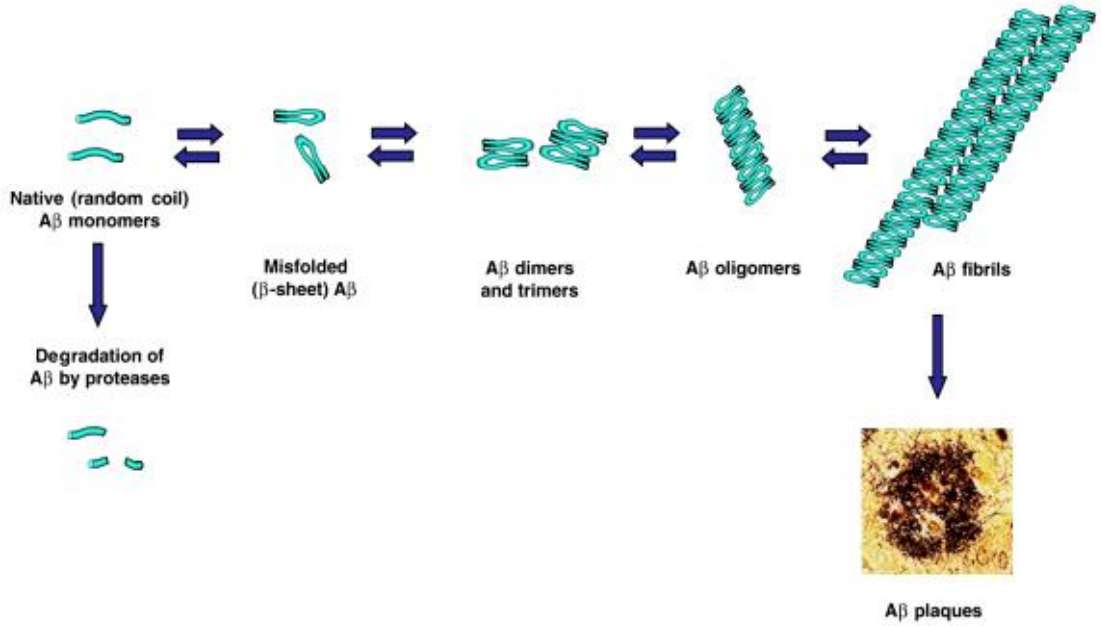

Figure 4 - Model for Aβ misfolding and aggregation [4].

Three main synaptotoxic effects of Aβ have been recognized: inhibition of long-term potentiation (LTP), removal of synaptic glutamate receptors and elimination of glutamate synapses (Figure 5) [22]. Glutamate synapses constitute 85-90% of the synapses in the mammalian cortex and their plasticity is thought to be the basis for learning and memory [22]. The postsynaptic membrane of the glutamate synapse is typically equipped with ionotropic AMPA and NMDA receptors [22]. The AMPA receptors are responsible for the normal, fast electrical signaling while the NMDA receptors, which are highly permeable for calcium, are required for the induction of LTP and its counterpart long-term depression (LTD) at these synapses [22]. LTP, a lasting increase in synaptic efficacy, typically involves an expansion of the synapse with more AMPA receptors, whereas the opposite is typical for LTD [22]. The inhibitory action of Aβ on NMDA receptor-dependent LTP has been shown in different experimental settings, including genetic modifications leading to overproduction of Aβ in human CSF and Aβ oligomers from AD brains [22].

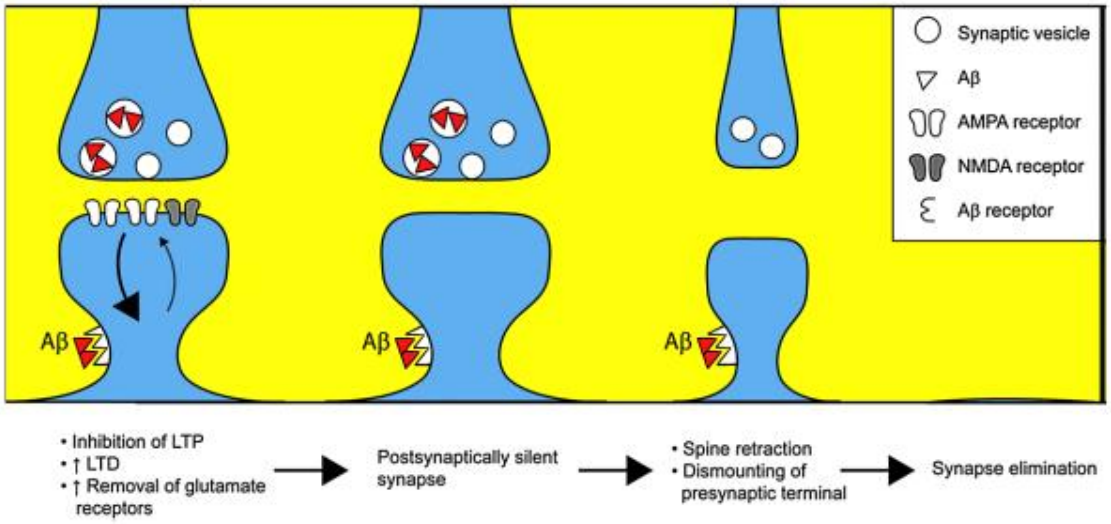

Figure 5 - Proposed model of Aβ-induced synaptotoxic effects and synapse elimination in AD [22].

2.3 Electrochemistry

Electrochemistry involves chemical phenomena associated with charge separation. Often this charge separation leads to charge transfer, which can occur homogeneously in solution, or heterogeneously on electrode surfaces [23]. Electrodes are linked by conducting paths both in solution (via ionic transport) and externally (via electric wires etc.) so that charge can be transported [23]. If the cell configuration permits, the products of the two electrode reactions can be separated.

Electroanalytical techniques analyze the relationship between the measurements of electrical quantities, such as current, potential, or charge, and the chemical parameters [24]. The oxidation/reduction process involves the exchange of electrons from one specie to another. Electrochemical processes take place at the electrode-solution interface [23, 25]. The electrochemical analyses usually require the use of three electrodes - the working electrode, reference electrode and counter electrode – and a contacting solution (electrolyte) containing the analyte [26]. The working electrode can be of various materials and geometries and gives response to the target analyte [26]. The electrode surface is thus a junction between an ionic conductor and an electronic conductor. The reference electrode has constant potential and is independent of the properties of the solution [26].

Different types of electrical signal used for quantification reflect the differences between electroanalytical techniques [11, 23, 25, 27]. Such electroanalytical measurements have been found to have a vast range of applications, where it could be highlighted the biomedical analysis.

The objective of controlled-potential electroanalytical experiments is to obtain a current response that is related to the concentration of the target analyte [25]. This objective is accomplished by monitoring the transfer of electron(s) during the redox process of the analyte:

$$O + ne^- \leftrightarrow R \qquad (1)$$

where O and R are the oxidized and reduced species, respectively. Electrode reactions are heterogeneous and take place in the interfacial region between electrode and solution, the region where charge distribution differs from that of the bulk phases [11, 23, 25, 27].

The resulting current-potential plot, also known as voltammogram, is a display of current signal versus the potential signal [28]. The exact shape and magnitude of the voltammetric response is controlled by the processes involved in the electrode reaction. The resulting current from a change in oxidation state of the electroactive species is termed the faradaic current because it obeys Faraday's law [23, 25]. The faradaic current is a direct measure of the rate of the redox reaction. The total current is a result of the sum of the faradaic currents for the sample and blank solutions, as well as the nonfaradaic charging background current [23, 25].

2.3.1. Mass transfer

Mass transfer is the movement of material from one location to another in solution. The rate of an electrode reaction is affected not only by the electrode itself but also by the transport of species to and from bulk solution [11, 23, 25]. It is important to consider the movement of ions in electrolyte solutions between anode and cathode as solvated ions move at different velocities, according to their size and charge. Diffusion is due to a concentration gradient, and migration to electric field effects [11, 23, 25]. Thus, whilst diffusion occurs for all species, migration affects only charged species (effectively, owing to the existence of dipoles, or induced dipoles in neutral species, a small electric field effect is observed) [11, 23, 25]. Forced convection considerably increases the transport of species. Natural convection, due to thermal gradients, also exists, but conditions where this movement is negligible are generally used [25].

In electrochemical systems, three modes of mass transport are generally considered (Figure 6):

• Diffusion: the spontaneous movement under the influence of concentration gradient that is from region of high concentration to region of lower concentration aimed at minimizing concentration differences [25].

• Convection: transport to the electrode by a gross physical movement; such fluid flow occurs with stirring or flow of the solution and with rotation or vibration of the electrode (forced convection) or due to density gradients (natural convection) [25].

• Migration: movement of charged particles along an electrical field [25].

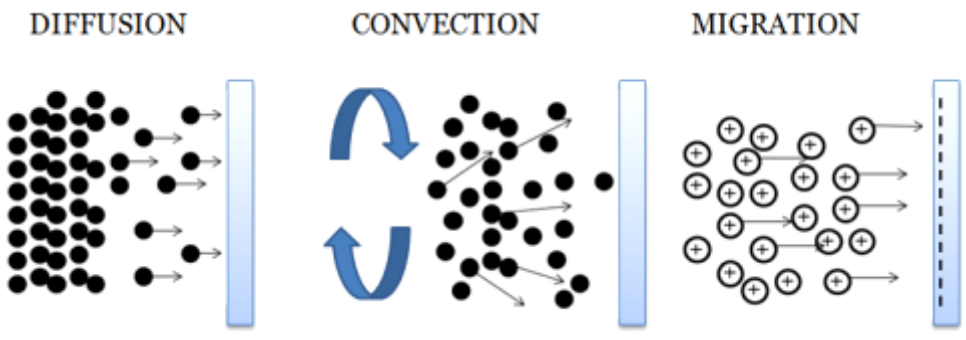

Figure 6 - Three methods for mass transfer in electrochemical systems [25].

2.3.2 The electrical double layer

The electrical double layer (Figure 7) is the array of charged particles and/or oriented dipoles that exists at every material interface. In electrochemistry, such a layer reflects the ionic zones formed in the solution to compensate for the excess of charge on the electrode. A positively charged electrode thus attracts a layer of negative ions (vice versa) [11, 23, 25, 27].

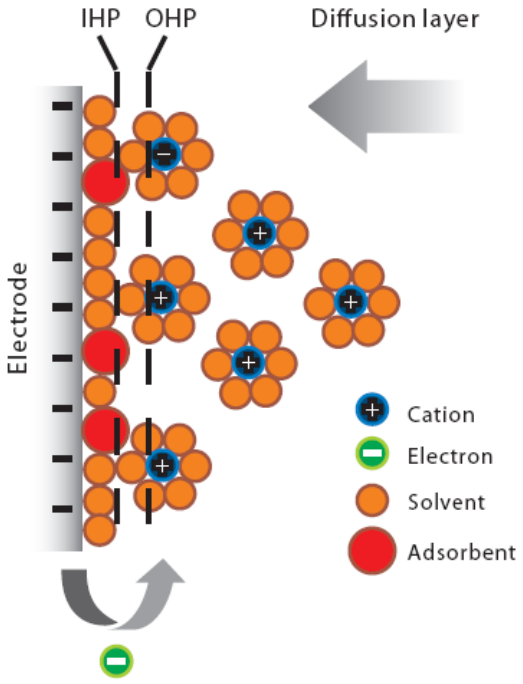

Figure 7 - Schematic representation of the electrical double layer. IHP-inner Helmholtz plane; OHP-outer Helmholtz plane [29].

The inner layer (closest to the electrode), known as the inner Helmholtz plane (IHP), contains solvent molecules and specifically adsorbed ions, which are not fully solvated [25]. It is defined by the locus of points for the specifically adsorbed ions. The next layer, the outer Helmholtz plane (OHP), reflects the imaginary plane passing through the center of solvated ions at their closest approach to the surface [25]. The solvated ions are nonspecifically adsorbed and are attracted to the surface by long-range coulomb forces [25]. Both Helmholtz layers represent the compact layer. Such a compact layer of charges is strongly held by the electrode and can survive even when the electrode is pulled out of the solution [23, 25]. However, the Helmholtz model does not take into account the thermal motion of ions, which loosens them from the compact layer [23, 25].

The outer layer, referred to as the diffuse layer, is a three dimensional region of scattered ions, which extends from the OHP into the bulk solution. Such an ionic

distribution reflects the counterbalance between ordering forces of the electrical field and the disorder caused by a random thermal motion [23, 25].

2.3.3 Electrode materials

The choice of an electrode material depends on a great extent on the useful potential range of the electrode in the particular solvent employed and the purity of the materials [11, 23, 25, 27]. The usable potential range is limited by one or more of the following factors: decomposition of the supporting electrolyte and electrode dissolution or formation of a layer of an insulating/semiconducting substance on its surface [23].

Additionally, solid electrodes can be adversely affected by poisoning through contact with solutions containing contaminants [11, 23, 27]. Of the many solid materials that can be used as working electrode the most frequently used are platinum, carbon and gold. One of the most important factors when working with solid materials is that the analysis is dependent of the surface state of the electrodes [23]. This way these electrodes need to go through a process of pretreatment and polishing to obtain reproducible results [23].

Gold is most often used as redox electrode for studying electron transfer kinetics and mechanism, and determining thermodynamic parameters, due in large part to its inertness [23, 27]. Still, in certain electrochemical conditions gold can be highly active [23]. A general advantage of metal electrodes is that their high conductivity results in low background currents [11, 23, 27]. Their surfaces can be modified by electrodeposition or chemical modification. Another advantage of the use of metal electrodes is the ease of construction of the electrode assembly, and ease of polishing [11, 23, 27]. At last, gold has unique properties to provide a suitable microenvironment for biomolecules immobilization retaining their biological activity, and to facilitate electron transfer between the immobilized proteins and electrode surfaces.

2.3.4. Electrochemical Techniques

2.3.4.1 Cyclic voltammetry

Cyclic voltammetry (CV) is the most used technique to obtain qualitative information about electrochemical reactions and it is often the first applied technique for the electrochemical study of a compound, a biological material, or an electrode surface [23-26]. The application of CV results from its capability for rapidly detect the redox behavior over a wide potential range and to provide information on kinetics of heterogeneous electron-transfer reaction and on coupled chemical reactions or adsorption processes [23-26]. It enables the electrode potential to be rapidly scanned in search of redox couples. Once located, a couple can be characterized from the potentials of peaks on the cyclic voltammogram and from changes caused by variation of the scan rate [23-25].

CV consists of cycling the potential of an electrode and measuring the resulting current [23, 25, 28]. The excitation signal for CV is a linear potential scan with a triangular waveform (Figure 8) [28, 30]. The potential excitation signal sweeps the potential of the electrode between two values, designed the switching potentials [28]. The excitation signal causes, in the first place, the potential to scan positively versus the reference electrode at which point the scan direction is reversed causing a negative scan back to the original value (Figure 8) [28].

The peak current for a reversible couple at a normal-sized planar electrode is described (at 298 K) by the Randles–Sevcik equation [30]:

$$\mathrm{i_p} = (2.69 \times 10^{-5})\mathrm{n}^{3/2}\mathrm{AD}^{1/2}\mathrm{v}^{1/2}\mathrm{c} \qquad (2)$$

where the peak current i_p is in amperes, n is the number of electrons transferred in redox events, the electrode area A is in cm^2, the diffusion coefficient D is in cm^2/s, v is in V/s and the bulk concentration of the reactant c is in mol/cm^3.

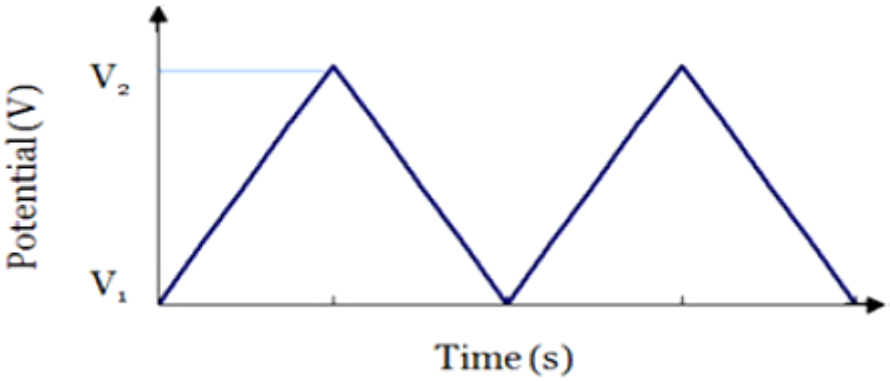

Figure 8 - Typical excitation signal for CV - a triangular potential waveform with switching potentials at V_1 and V_2 [31].

2.3.4.2 Square-wave voltammetry

Square-wave voltammetry (SWV) is a further improvement of staircase voltammetry, which is itself a derivative of linear sweep voltammetry [23, 25, 26, 32]. In linear sweep voltammetry the current at a working electrode is measured while the potential between the working electrode and a reference electrode is swept linearly in time. SWV is a large amplitude differential technique in which a waveform is composed by symmetrical square waves [23, 25, 26]. The excitation signal in SWV (Figure 9) consists of a symmetrical square-wave pulse of amplitude superimposed on a staircase waveform, where the forward pulse of the square wave coincides with the staircase step [23, 25, 26]. The current is sampled twice during each square-wave cycle, once at the end of the forward pulse and once at the end of the reverse pulse. The current is measured at the end of each potential change so that the contribution to the current signal from the capacitive charging current is minimized [25, 32]. The net current is obtained by taking the difference between the forward and reverse currents and is centered on the redox potential [25]. The peak height is directly proportional to the concentration of the electroactive species and direct detection limits as low as 10^{-8} mol/L are possible [23, 25]. The fact that net current is large compared to either forward or backward current and coupled with effective discrimination against the charging current, allows the achievement of excellent sensitivity in SWV [24, 25].

SWV has several advantages, namely excellent sensitivity and the minimization of background currents [23-26]. One of the major advantages is also its speed [24]. The effective scan rate is of the order of 500 mV/s and as a result, the analysis time is drastically reduced [24]. Frequencies of 1 to 100 square-wave cycles per second permit

the use of extremely fast potential scan rates [24]. The analysis time is reduced and a complete voltammogram can be recorded within a few seconds [24]. Another advantage of this technique is the minimization of oxygen interference. In stripping voltammetry during the preconcentration step the dissolved oxygen is irreversibility reduced at potentials sufficiently negatives and it is depleted from the electrode surface. During the stripping step at elevated scan rates and high frequencies, oxygen does not have enough time to reach again the electrode surface. The detection limits of this technique can be compared to those of chromatographic and spectroscopy techniques [23, 25, 32].

SWV is the most used voltammetric technique for quantification and it is applied in the study of electrode kinetics with regard to preceding, following, or catalytic homogeneous chemical reactions, determination of some species at trace levels, and it is used with electrochemical detection in HPLC [23, 25, 33].

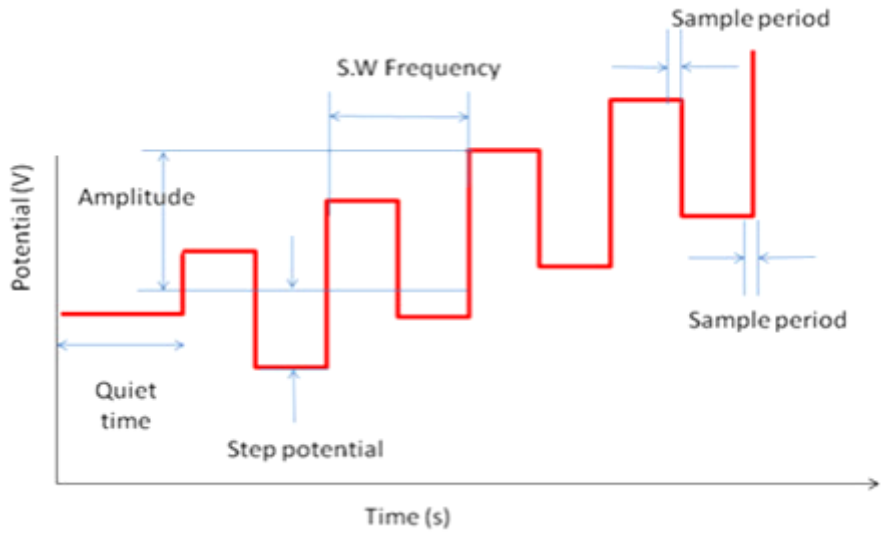

Figure 9 - Schematic waveform for square-wave voltammetry [31].

2.3.4.3 Electrochemical Impedance Spectroscopy

Electrochemical Impedance Spectroscopy (EIS) or AC impedance methods have seen tremendous increase in popularity in recent years [34]. Initially applied to the determination of the double layer capacitance, they are now applied to the characterization of electrode processes and complex interfaces [34]. EIS studies the system response to the application of a periodic small amplitude AC signal. These measurements are carried out at different AC frequencies and analysis of the system response contains information about the interface, its structure and reactions taking place there [34]. By varying the excitation frequency of the applied potential over a range of frequencies, one can calculate the complex impedance, sum of the real and imaginary impedance components, of the system as a function of the frequency (*i.e.* angular frequency, *w*) [35]. Therefore, EIS combines the analysis of both real and imaginary components of impedance, namely the electrical resistance and reactance [29, 34, 35].

EIS possesses the ability to study any intrinsic material property or specific processes that could influence the conductivity/resistivity or capacitivity of an electrochemical system. Therefore, EIS is a useful tool in the development and analysis of materials for biosensor transduction, such as the study of polymer degradation [35]. However it is a complementary technique and other methods must also be used to elucidate the interfacial processes [34, 35].

The electric equivalent circuit first proposed by Randles, shown in figure 10, is commonly used in EIS for interpretation of impedance spectra [29]. It includes a solution resistance (R_s), a double layer capacitor (C_d) and a charge transfer (R_{ct}) or polarization resistance (R_p). When the charge transfer takes place at the interface, the mass transports of the reactant and product take on roles in determining the rate of electron transfer, which depends on the consumption of the oxidants and the production of the reductant near the electrode surface [29]. The mass transport of the reactants and the products provides another class of impedance, Warburg impedance (Z_W), which can be exploited by electroanalytical chemists because it shows up in the form of a peak current in a voltammogram or a current plateau in a polarogram [29].

In addition, to be a useful model in its own right, the Randles model is the starting point for other more complex models [29]. The double layer capacity is parallel with the impedance due to the charge transfer reaction [29]. Figure 10 shows an example of a Nyquist plot for a Randles cell. The solution resistance can be found by

reading the real axis value at the high frequency intercept, which is the intercept near the origin of the plot [29]. The value at the right side of the real axis (low frequency region) is the sum of the charge transfer resistance and the solution resistance [29]. The intermediate-frequency component (*circle*) arising from the R_p and C_d is located in between [29]. In a simple situation, the Warburg element manifests itself in EIS spectra by a line with an angle of 45 degrees in the low frequency region [29].

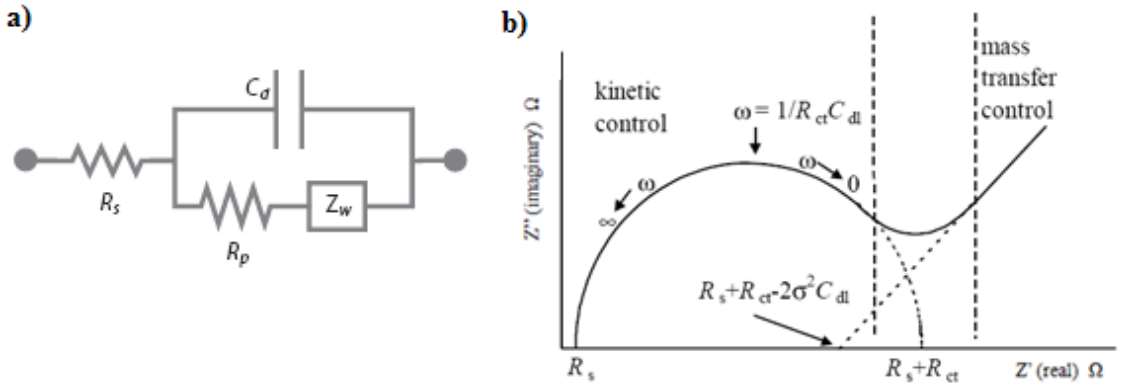

Figure 10 - a) A schematic diagram of an idealized Randles electrical equivalent circuit [29]; b) Nyquist plot showing the high and low frequency components [34].

For electrochemical sensing, impedance techniques are useful to monitor changes in electrical properties arising from biorecognition events at the surfaces of modified electrodes. For example, changes in the conductivity of the electrode can be measured as a result of protein immobilization and antibody-antigen reactions on the electrode surface [35].

EIS has become a mature and well understood technique. It is now possible to acquire, validate and quantitatively interpret the experimental impedances. However, the most difficult problem in EIS is modeling of the electrode processes. There is almost an infinite variety of different reactions and interfaces that can be studied (corrosion, coating, conducting polymers, batteries and fuel cells, etc.) and the main effort is now applied to understand and analyze these processes [35].

2.4 Biosensors

Biosensors are, by definition, sensing devices including a biological component (enzyme, antibody, animal or plant cell, oligonucleotide, lipid, microorganisms, etc.) intimately connected to a physical transducer (electrode, optical fiber, vibrating quartz, etc.) (Figure 11) [35, 36]. This dual configuration permits a quantitative study of the interaction between the analyte and an immobilized biocomponent [36, 37]. Designed for the purpose, biosensors are generally highly selective due to the possibility to tailor the specific interaction of compounds by immobilizing biological recognition elements on the sensor substrate that have a specific binding affinity to the desired molecule [35-38]. Typical recognition elements used in biosensors are: enzymes, antibodies, nucleic acids and cells. Ideally, biosensors should be readily implemented and allow for low reagent and energy consumption [35, 36, 39-42].

Nowadays, a lot of biosensors can be found in laboratories around the world but only one is known by its great ratio efficiency/cost and that is the glucose sensor. The major limitation, in several cases, in developing sensing devices is associated with the ability to miniaturize the transduction principle and the lack of cost-effective production method [37, 41]. Biosensors have an important role due to their inherent advantages as robustness, easy miniaturization, excellent detection limits, possibility of using small analyte volumes, and ability to be used in turbid biofluids with optically absorbing and fluorescing compounds [35].

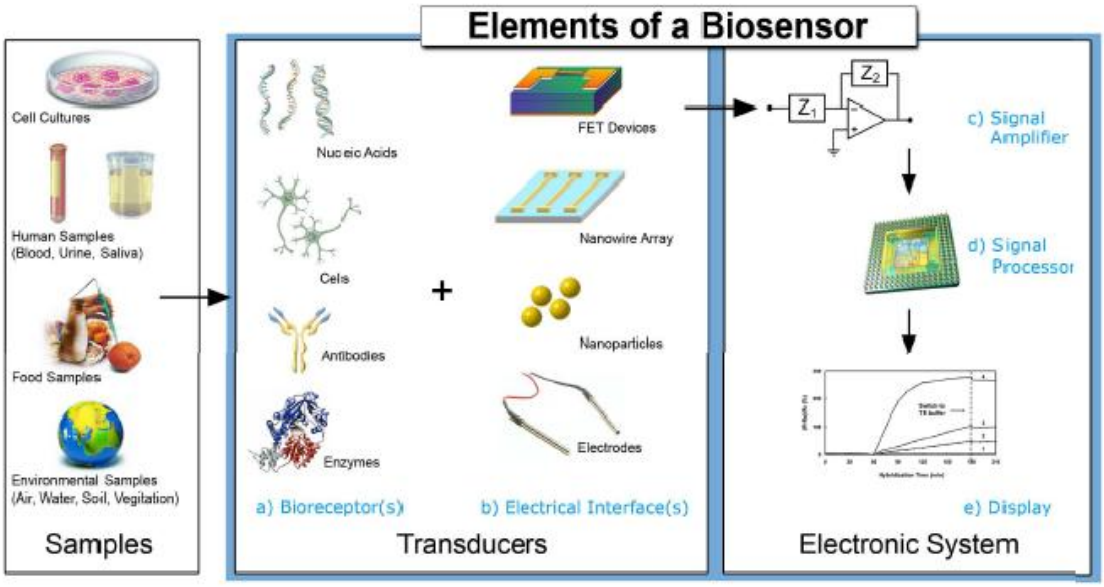

Figure 11 - Components of typical biosensor [35].

In order to construct a successful biosensor a number of conditions must be met [35]:

1. The biocatalyst must be highly specific for the purpose of the analysis, be stable under normal storage conditions and show a low variation between assays.
2. The reaction should be as independent as manageable of such physical parameters as stirring, pH and temperature. This will allow analysis of samples with minimal pre-treatment. If the reaction involves cofactors or coenzymes these should, preferably, also be co-immobilized with the enzyme.
3. The response should be accurate, precise, reproducible and linear over the concentration range of interest. It should also be free from electrical or other transducer induced noise.
4. If the biosensor is to be used for invasive monitoring in clinical situations, the probe must be tiny and biocompatible, having no toxic or antigenic effects. Furthermore, the biosensor should not be prone to inactivation or proteolysis.
5. For rapid measurements of analytes from human samples it is desirable that the biosensor can provide real-time analysis.
6. The complete biosensor should be cheap, small, portable and capable of being used by semi-skilled operators.

2.5 Electrochemical immunosensors

Immunosensors are affinity ligand-based biosensing devices that couple immunochemical reactions to appropriate transducers [43]. In recent decades, immunosensors have received rapid development and wide applications with various detection formats. The general working principle of the immunosensors is based on the fact that the specific immunochemical recognition of antibodies (antigens) immobilized on a transducer to antigens (antibodies) in the sample media can produce analytical signals dynamically varying with the concentrations of analytes of interest [43-45]. The merits of immunosensors are related to selectivity and affinity of the antibody-antigen reaction [46]. Here, the highly specific binding between the antibody and the antigen involves different types of interaction forces, basically hydrophobic and electrostatic interactions, van der Waals forces and hydrogen bonding. The antigen–antibody reaction is reversible and, owing to the relative weakness of the forces holding the antibody and antigen together, the complex formed would dissociate in dependence upon the reaction environment (e.g. pH and ion strength) [43]. High specificity is achieved by the molecular recognition of target analytes (usually the antigens) by antibodies (biological recognition element) to form a stable complex on the surface of an immunoassay system or an immunosensor [40, 43, 47-49]. On the other hand, sensitivity depends on several factors including the use of high affinity analyte-specific antibodies, their orientation after being immobilized on the immunoassay or immunosensor surface and the appropriate detection system for measuring the analytical signal [48, 49]. This recognition reaction defines the high selectivity and sensitivity of the transducer device [43]. The electronic part is used to amplify and digitalize the physicochemical output signal from the transducer devices such as electrochemical (potentiometric, conductometric, capacitative, impedance, amperometric), optical (fluorescence, luminescence, refractive index), and microgravimetric devices [43].

Electrochemical immunosensors have been applied to several fields of science including medical diagnosis [44, 45, 50], environmental analysis [51, 52] and biological process monitoring [53]. In the biological area, considerable efforts have been devoted to the development of precise, rapid, sensitive, and selective immunosensors by measurement of the markers or pathogenic microorganisms responsible for the diseases, such as proteins, enzymes, viruses, bacteria, and hormones [47, 54-57]. This technology gains practical usefulness from a combination of selective biochemical recognition with

the high sensitivity of electrochemical detection [58]. With the development of technology, such biosensors profit from miniaturized electrochemical instrumentation and are thus very advantageous for some sophisticated applications requiring portability, rapid measurement and use with a small volume of samples [58]. Several reviews confirm the attractive advantages of electrochemical biosensors [9, 10, 59-62].

2.5.1 The antibody-antigen interaction

The fundamental basis of all immunosensors is the specificity of the molecular recognition of antigens by antibodies to form a stable complex. Antibodies are a family of glycoproteins known as immunoglobulins (Ig). There are generally five distinct classes of glycoproteins (IgA, IgG, IgM, IgD, and IgE) with IgG being the most abundant class (approximately 70%) and most often used in immunoanalytical techniques [48, 63]. IgG is a "Y"-shaped molecule based upon two distinct types of polypeptide chains (Figure 12). The molecular weight of the smaller (light) chain is approximately 25 kDa, while that of the larger (heavy) chain is approximately 50 kDa. In each IgG molecule, there are two light and two heavy chains held together by disulfide linkages [48, 63].

Antibodies show very high specificity and binding constants toward their corresponding antigens. An antigen has been defined as any agent that gives rise to antibody formation specific for that agent when transferred to a living cell system containing cells of the immunologically competent type [48, 63].

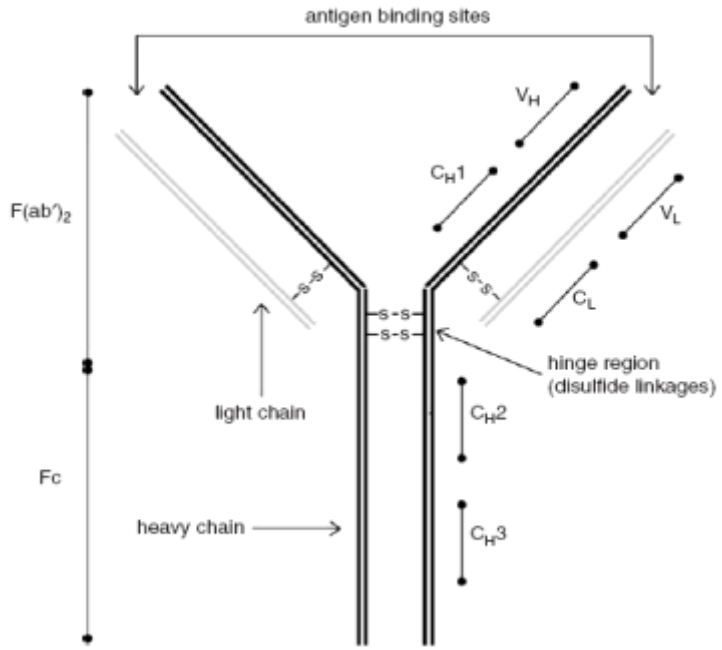

Figure 12 - A schematic illustrating the "Y"-shaped structure of an antibody [48].

2.5.2 Immunoassays

Immunoassay is the predominant analytical technique for quantitative measurements, being used over a wide range of concentrations, in many different biological matrices, and in a range of delivery formats. Immunoassays are the quantitative methods of analysis where antibodies are the primary binding agents for the antigen (which is often the analyte) of interest [9, 43, 46, 48].

All immunoassays depend on measuring the fractional occupancy of the recognition sites. Usually, immunoassays are heterogeneous, which means that either the antibody or the antigen is immobilized on a solid carrier and an immunocomplex is formed upon contact with a solution containing the other immunoagent while homogeneous immunoassays take place in the solution phase. Compared to homogeneous immunoassays, the heterogeneous immunoassays are easily designed and constructed. The unbound proteins are removed by washing and the response obtained from the labels is proportional to the amount of protein bound. However, such a measurement can rely on either the evaluation of occupied sites or, indirectly, on measuring unoccupied sites. This leads to the development of either a "competitive" or a "non-competitive" immunoassay format [46, 48].

In a competitive immunoassay (Figure 13), unlabeled analyte in the test sample is measured by its ability to compete with the labeled antigen for a limited number of

antibody-binding sites [46, 48]. In electrochemical immunoassays, an enzyme label or an electroactive label is commonly used. Quantitative analysis can be achieved by determining the amount of labeled analyte that interacted at the binding sites [48]. Therefore, with a fixed number of antibody sites, a smaller signal is expected when the ratio between the quantities of sample to labeled analyte is large [48]. In contrast, a larger signal is obtained when there is a small quantity ratio. Therefore, the signal produced by the bound labeled analyte is usually inversely proportional to the amount of sample analyte [46, 48].

Non-competitive immunoassays (also known as a "sandwich" immunoassay) give the highest level of sensitivity and specificity because of the use of a couple of match antibodies. In this format the sample analyte is captured by an excess of a capture antibody, separating it from the bulk sample [48]. The captured analyte is then exposed to an excess of second signal antibody (secondary antibody (Ab_2)), which will only bind to the existing capture antibody-analyte complex [48]. This structure is a classic two-site immunoassay complex in which the analyte is sandwiched between two antibodies (Figure 13). High-affinity antibodies and appropriate labels are usually employed for the amplification of electrochemical signal [46, 48]. Enzyme-labeled antibodies are often used as detection antibodies that result in amplification of the measurement signal [46, 48]. In an ideal non-competitive immunoassay, no signal would be produced in the absence of any analyte because there are no appropriate sites available for binding to the signal antibody [48]. However, in practice, this is not the case due to nonspecific interactions between the signal antibody and other components of the immunoassay [48]. Therefore, it is always desirable to use a blocking reagent to reduce these nonspecific interactions. Nonspecific adsorption also needs to be considered when determining the quantity of signal antibody for use in a system [48]. Although this immunoassay format often offers superior specificity, it can only be used for the quantification of analytes with two antigenic determinants that can be simultaneously recognized [46, 48]. Several studies using both competitive and non-competitive immunoassays have been reported [64-67].

Electrochemical detection of immunointeraction can be performed both with and without labeling. A frequently used format in electrochemical immunosensing is an amperometric immunosensor, where proteins are labeled with enzymes producing an electroactive product from an added substrate [9].

Direct detection without labeling can be performed by cyclic voltammetry, chronoamperometry, impedimetry, and by measuring the current during potential pulses (pulsed amperometric detection). These methods are able to detect a change in capacitance and/or resistance of the electrode induced by binding of protein. These immunosensors have been developed using various substrates [9].

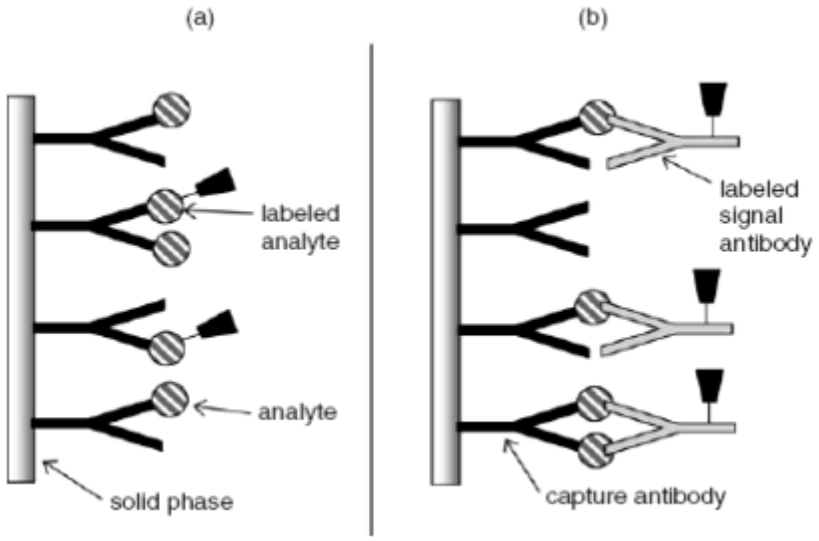

Figure 13 - Schematic representation of (a) competitive and (b) non-competitive immunoassay formats [48].

A critical issue in immunoassays is minimization of nonspecific binding (NSB) of interfering species in samples such as serum or blood, as well as NSB of the labeled Ab_2 that arises when this signal producing species is bound to non-antigen sites on the sensor [68]. In labeled assays, non-enzyme Ab_2 bound to sites other than the analyte protein still gives a signal, but it is not proportional to the analyte protein concentration. This can increase detection limits and degrade sensitivity [68]. NSB is usually minimized by washing with a cocktail that includes casein or bovine serum albumin and detergents in NSB blocking steps. Another solution consists in tailoring the sensor surface with appropriate chemical groups that can also inhibit protein adsorption, and one of the most effective surfaces features polyethylene glycol (PEG) moieties [69, 70]. Such functionalized surfaces, although useful, may still permit small amounts of NSB that could significantly increase background in the pg to ng/mL analyte concentration ranges [68].

2.5.3 Antibody immobilization techniques

Since immunosensors usually measure the signals resulting from the specific immunoreactions between the antigens and the antibodies, it is clear that the immobilization procedures of the antibodies on the surfaces of transducers should play an important role in the construction of immunosensors.

The manner in which a capture antibody is immobilized on a solid phase is a critical aspect that requires careful consideration in the design of an immunoassay system, whether it is competitive or non-competitive. A desirable feature of the chosen method is that it results in an immobilized capture antibody that is oriented with minimal steric hindrance to interact favorably with its target antigen. Equally important, it is highly desirable to immobilize the antibody without a significant change in its ability to bind its antigen. Clearly, all these features have a direct bearing on the level of sensitivity and dynamic range achievable by an immunosystem. There are several strategies for immobilizing a capture antibody on a solid phase including covalent attachment, physical adsorption or electrostatic/physical entrapment in a polymer matrix. These commonly used immobilization strategies are described below [48].

2.5.3.1 Biotin-(strept)avidin interaction

Specific affinity interactions for antibody immobilization have been widely used in immunoassay systems in recent years. The (strept)avidin–biotin interaction is one such example. This technique may be used to immobilize various types of biomolecules such as nucleic acids, polysaccharides and proteins, including the capture antibody in immunoassay/immunosensor systems. The technique usually involves biotinylating the capture antibody and coating a solid phase with either avidin or streptavidin [48, 71].

The avidin-biotin and biotin–streptavidin interactions are the strongest known non-covalent interactions, presenting dissociation constants of the order of 10^{-15} mol/L, between a protein and ligand [72]. The complexes formations are very rapid, and once formed withstand high temperatures, pH variations, and are resistant to dissociation when exposed to chemicals such as detergents and denaturing agents [48, 73]. Equally important, the use of this immobilization technique maintains the biological function of the immobilized antibody. In some cases, neutravidin, which is an almost neutrally charged variation of avidin, is used to minimize any non-specific binding by charged species to maintain high binding affinity for biotin [48, 71].

Despite the several mentioned advantages the biotin-(strept)avidin complex is not amenable to multiplex experiments. Because any biotinylated molecule will bind to any biotin-binding protein, these reagents must be used in combination with other detection-probe systems (i.e., primary-secondary antibodies) for multiplex experiments. Also, because biotin is a biological molecule, endogenous biotin can cause background and specificity issues when performing assays with certain biotin-rich tissues and extracts (i.e., brain, liver, milk, eggs, corn). In addition, the strength of the interaction between biotin and avidin may also influence the application for which this binding is required, as the harsh conditions required to break the avidin-biotin bonds may denature target proteins.

2.5.3.2 Antibody-binding proteins

Another commonly used affinity-based immobilization technique for capture antibodies in immunoassay systems involves a bacterial antibody-binding protein. Protein A and Protein G are the two most common [48]. These proteins bind specifically to antibodies through their non-antigenic (Fc) regions, which allow the antigen binding sites of the immobilized antibody to be oriented away from the solid phase and be available to bind the target analyte. As these proteins interact directly with the Fc region of antibodies, there is no need for antibody biotinylation [48].

Protein A has a molecular weight of approximately 42 kDa and was originally isolated from the cell wall of *Staphylococcus aureus* [74]. It is known to contain five Fc binding domains located towards its -NH_2 terminal [48]. Optimal binding occurs at pH 8.2, although binding is also effective at neutral or physiological conditions (pH 7.0 to 7.6). However, the interaction between Protein A and IgG is not equivalent for all species. Even within a species, Protein A interacts with some subclasses of IgG and not others [48]. The binding capacity of Protein A is limited to three human IgG subclasses (IgG 1, 2 and 4) [75]. Also, Protein A will not bind to goat and rat IgG, and only weakly to mouse IgG [76].

The second bacterial antibody binding protein, Protein G, is a cell surface protein of group C and G *streptococcus* with three Fc binding domains located near its C-terminal, and has specificity for subclasses of antibodies from many species [75]. Optimal binding occurs at pH 5.0, although binding is also effective at pH 7.0 to 7.2. Protein G has greater affinity than Protein A for most mammalian IgGs. However there are inconsistencies in reported binding properties of IgG to Protein G. Variations in

isolation and manufacturing methods for Protein G may affect IgG binding, partially because there are differing numbers of IgG-binding sites on various sources of Protein G [48].

Differences in binding characteristics between Protein A and Protein G may be explained by the different compositions in the IgG-binding sites of each protein. The tertiary structures of these proteins are very similar although their amino acid compositions are significantly different [48].

2.5.3.3 Conducting polymers

Conducting polymers such as polyaniline, polypyrrole, and polythiophene are commonly applied for immobilizing capture antibodies in immunoassay systems [48, 77]. The polymers can be used in amperometric, potentiometric and impedimetric immunoassay systems [48, 77, 78]. Conducting polymers may provide a direct route of electron transfer between an enzyme and the electrode surface and, where required, negate the need for a mediator to shuttle electrons between the enzyme and the electrode [48]. Conducting polymers may also facilitate "reagentless" or "label-free" immunosensing [48]. A common way to immobilize antibodies involving conducting polymers is entrapment within the polymeric chains [77]. The antibody is usually co-immobilized with the polymer onto the sensor surface from a monomer solution containing the antibody [48]. However, entrapment may result in denaturation of the antibody, leading to a loss of activity [48]. Furthermore, a large proportion of the immobilized antibody will be trapped within the polymer matrix and is thus inaccessible for binding to its antigen [48]. An alternative to entrapment is covalent attachment of the antibody to active groups on a pre-immobilized conducting polymer film [48, 77].

2.5.3.4 Antibody fragments

Sometimes it is useful to study or make use of the activity of one portion of an immunoglobulin without interference from other portions of the molecule. It is possible to selectively cleave the immunoglobulin molecule into fragments that have discrete characteristics. Fragmentation of an antibody is usually achieved enzymatically with proteolytic enzymes such as chymotrypsin, trypsin, and papain that digest or cleave certain portions of the immunoglobulin protein structure [48, 79].

The two groups of antibody fragments of primary interest are (a) antigen-binding fragments such as F(ab')2 and (b) class-defining fragments such as Fc that do not bind

antigen [80]. Several types of antigen-binding fragments are possible, but each contains at least the variable regions of both heavy and light immunoglobulin chains (V_H and V_L, respectively) held together (usually by disulfide bonds) so as to preserve the antibody-binding site [80]. Fc fragments consist of the heavy chain constant region (Fc region) of an immunoglobulin and mediate cellular effector functions [80].

Following enzymatic digestion, the disulfide linkages holding the two chains of the resulting $F(ab')_2$ fragment together are typically reduced with reagents such as dithiothreitol or 2-mercaptoethalamine [48]. This results in two Fab' fragments, each with a terminal thiol group. The fragments thus have a high affinity for a gold surface, on which they can therefore self-assemble without the need of any additional reagent [48]. The resulting layers have an ordered arrangement with the antibody-binding regions being oriented in such a way that they are more accessible to bind antigen [48].

2.5.3.5 Self-assembled monolayers

Many physical and chemical methods for immobilizing proteins and enzymes on solid surfaces, like adsorption and entrapment within membranes, are used. However, these techniques present some problems such as conformational change affecting the functional activity, adsorption with random orientation, detachment of the protein and fragility of the membrane resulting in less sensitivity and short longevity [43, 81]. Thus, there is an ever increasing demand for assembly techniques for immobilizing protein on the electrode surface. The well-characterized self-assembled monolayers (SAMs) on metal electrodes have been widely used as a new strategy for the immobilization, orientation and molecular organization of biomolecules at interfaces [81]. The term ‘‘self-assembly’’ refers to the spontaneous arrangement of discrete nanometre-sized units from simpler subunits or building blocks into an ordered or even aggregate of functional entities towards an energetically stable form [82, 83]. During the self-assembly process, the constituent subunits (atoms, molecules, biomolecules, simple biological structures, etc), combine in such a way that they form a secondary, more complex structure with fewer degrees of freedom [82]. In other words, SAMs are organic assemblies formed by the adsorption of molecules (or atoms) on solid surfaces in which intermolecular forces play a key role and which can be spontaneously formed from solution or from vapor phase [82, 84, 85].

The stability of the bond between the specific functional group of a reagent and the electrode surface over a wide range of applied potentials and the well-defined

microenvironment mimicking biological membranes make such a system suitable for orienting proteins without denaturation and facilitating the electron transfer of proteins [86]. In addition, the strong inter-chain interactions (van der Waals interactions) ensure tight packing and stability of monolayers leading to several applications including chemical sensing [87], control of surface properties such as wettability and friction [84, 88], corrosion protection [89, 90], stabilization and functionalization of nanosized objects (nanoparticles, nanorods, nanowires) [84, 91, 92], patterning [93] and semiconductor passivation [94].

Each of the molecules that constitute the building blocks of the system can be divided into three different parts (Figure 14): the headgroup (linking group), the backbone (main chain), and the specific terminal (active) group [82, 84]. The headgroup guides the self-assembly process on each type of substrate, linking the hydrocarbon chain (of variable length) to the metal surface through a strong bond; in many cases, the headgroup also has a high affinity for the surface and displaces adsorbed acidental organic materials from the surface [82]. The interactions among backbone hydrocarbon chains (involving van der Waals and hydrophobic forces) ensure an efficient packing of the monolayer and contribute to stabilize the structures with increasing chain length. This section of the molecule can also act as a physical barrier and alters electronic conductivity and local optical properties [82, 84]. The terminal group determines specific surface properties (hydrophilic, hydrophobic), and can also be used to anchor different molecules, biomolecules, or nanostructures by weak interactions or covalent bonds [82, 84, 85].

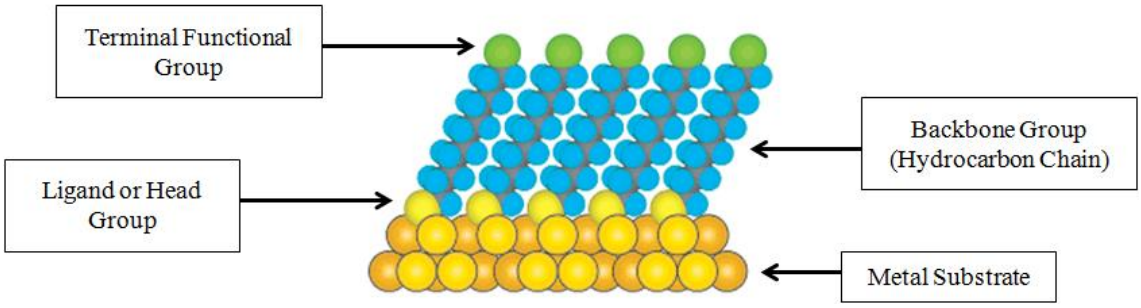

Figure 14 - Schematic diagram of an ideal, single-crystalline SAM of alkanethiolates supported on a gold surface. The anatomy of the SAM is highlighted [84].

Formation of SAM is essentially an organization of molecules that arrange themselves spontaneously on solid or liquid surfaces into crystalline (or semicrystalline)

structures, offering one of the most elegant approaches towards making ultrathin organic films of controlled thickness [84, 87, 95]. Thus, SAM represents an easy way to provide a convenient, flexible, and simple system to tailor the interfacial properties of metals, metal oxides, and semiconductors and link materials with totally different physical and chemical properties [82, 84]. The main objective is to attain the capability of assembling individual molecules into highly ordered architectures for obtaining a desired function [82, 84].

The ease of preparation and the fact that it is possible to prepare SAMs with different terminal groups has converted them to the most important type of organic monolayer [82]. Also, SAMs can be formed not only on planar surfaces, but on objects of all sizes and with a variety of shapes [82]. Among SAMs, the most important and most extensively studied, because of their promising and current applications in several fields of nanotechnology are derived from the adsorption of alkanethiols on noble and coinage metals [84]. In addition, SAMs of arenethiols, alkanedithiols, arenedithiols are also studied but to a lesser extent [84]. Other SAMs on metals include those of dialkyldisulfides, and dialkylsulfides [84].

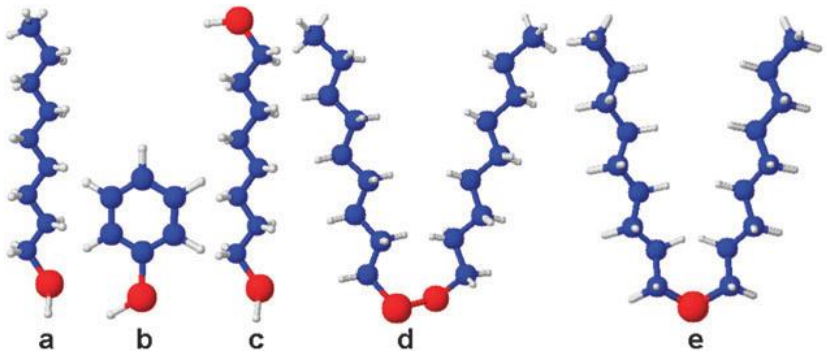

Figure 15 - Examples of sulfur compounds that form self-assembled monolayers on metals and semiconductors: (a) alkanethiol; (b) arenethiol; (c) alkanedithiol; (d) dialkyldisulfide; (e) dialkylsulfide. Red: sulfur atom, blue: carbon atom, white: hydrogen atom [82].

Thiol and dithiol SAMs on metals, and particularly on gold, have attracted considerable attention due to their easy preparation from gas phase or from solution, and their relatively high stability mediated by the strength of the S–Au bond and by van der Waals interactions [82]. These monolayers exhibit molecular order, and are relatively stable in ambient conditions. The high affinity of thiols for the surfaces of noble and coinage metals makes it possible to generate well-defined organic surfaces with useful and highly alterable chemical functionalities displayed at the exposed interface [82, 84].

A thiol molecule consists of three parts (Figure 16): (1) the sulfur headgroup, which forms a strong, covalent bond with the substrate, (2) the hydrocarbon chain (of variable length), which stabilizes the SAM through van der Waals interactions, and (3) the terminal group, which can have different functionalities [82]. A small change in the endgroup can be enough to change the physical and chemical properties of the layer [82, 84, 96]. Thus, $–CH_3$ and $–CF_3$ groups turn the SAM surface hydrophobic, metallophobic [82, 89] and highly anti-adherent, while –COOH, $–NH_2$ or –OH groups yield hydrophilic surfaces with good metal ion and protein binding properties [82, 97]. On the other hand, dithiols can be regarded as –SH-terminated thiols, and are very important to bind metallic ions and nanoparticles to the SAMs [84].

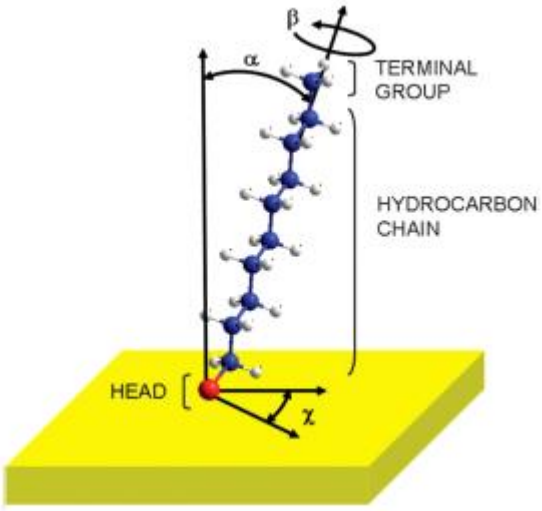

Figure 16 - Scheme of a decanethiol molecule adsorbed on gold. Red: sulfur atom; blue: carbon atom; white: hydrogen atom [82].

Self assembly of thiols and dithiols on gold is, in principle, easy to perform and can be done both in gas and liquid phase, the latter being the most popular method because of its simplicity and accessibility in most laboratories [82]. There are, however, a number of experimental factors that can affect the structure of the resulting SAM and the rate of formation: solvent, temperature, concentration of adsorbate, immersion time, purity of the adsorbate, concentration of oxygen in solution, cleanliness of the substrate, and chain length [84, 87]. This way and as a result of numerous studies it was concluded that, in general, adsorption is performed in ~1–10 mM solutions of thiols, dithiols, dialkyldisulfides and dialkylsulfides in different solvents, depending on the nature of the molecule [84]. Adsorption time also depends on the nature of the molecule: while 2–12 h are enough to form a well-ordered SAM in the case of long

chain alkanethiols, at least 24 h are necessary for short chain alkanethiols or thiols with certain endgroups different from $–CH_3$ [82].

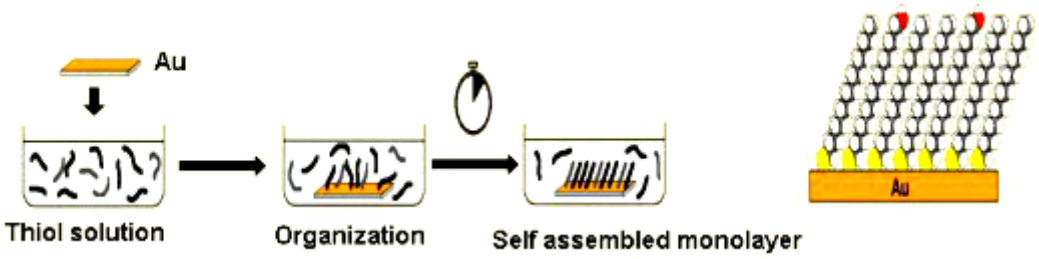

Figure 17 - The formation process of self-assembled monolayers.

The assembly process (Figure 17) starts with a physisorption step, followed by chemisorption of the molecules, and finally the formation of crystalline, ordered domains with molecules in a closed-packed configuration [82, 84, 85].

2.5.4 Nanomaterials based immunosensors

The unique properties of nanoscale materials and the ability to tailor their size and structure offer excellent prospects for designing highly sensitive and selective bioassays of nucleic acids and proteins, and render them applicable in the fields of medical imaging and therapy [8, 98]. Nanostructured materials are interesting tools with specific physical and chemical properties due to quantum-size effects and large surface areas, which provide them unique and different properties compared to bulk materials. Currently, the most intense research involves applying nanomaterials in immobilization [99]. Nanostructured sensor surfaces allow the improvement of biosensors properties and additional increases in their sensitivity by providing high surface areas enabling attachment of a large number of capture antibodies and by facilitating better access of protein analytes to these antibodies, enhancing the performance of bioassays [8, 68, 98, 100-102].

Nanotechnology has generated new innovative materials such as nanoparticles [103, 104], quantum dots [105, 106], nanowires [107, 108] and nanotubes [109, 110], all having unique properties applicable in delivering enhanced loading of biological elements, their increased stability or specificity, and enabling the use of novel transduction schemes. Several studies have reported about the enhancement of electronic properties when metallic nanostructures are used as components for electrodes modification [68, 101, 102].

Nanoparticles of different compositions and dimensions have been widely used in recent years as versatile and sensitive tracers for the electronic, optical, electrochemical and microgravimetric transduction of different biomolecular recognition events. The enormous signal enhancement associated with using nanoparticle amplifying labels and with forming nanoparticle-biomolecule assemblies provides the basis for ultrasensitive detection [68, 98, 101, 102, 111, 112]. Typically, metallic nanoparticles are prepared by chemical reduction of the corresponding transition metal salts in the presence of a stabilizer (often citrate, phosphanes or thiols) which binds to their surface to impart high stability and rich linking chemistry and provide the desired charge and solubility properties [98]. In the case of labile anionic ligands capping layers such as citrate or lipoic acid, the biomolecules are often coupled through noncovalent electrostatic interactions [101]. Nanoparticle labels in immunoassays were first reported by Dequaire *et al.* [113]. Metals in the nanoparticles served as labels after dissolution of the particles. After the antibodies capture of analyte proteins, Ab_2-nanoparticles were added to bind to them, and a NSB blocking wash was done. Then, the nanoparticles were dissolved in acid to produce high concentrations of electroactive metal ions. With gold nanoparticle-Ab_2 labels, Au^{3+} released by acid dissolution was detected by anodic stripping voltammetry to give a 3 pmol/L detection limit for IgG in buffer. Gold nanoparticles (AuNPs) have received great attention due to their attractive electronic, optical, and thermal as well as catalytic properties and potential applications in the fields of physics, chemistry, biology, medicine, and material science [114-119]. Therefore the synthesis and characterization of AuNPs have attracted considerable attention from a fundamental and practical point of view.

The preparation of AuNPs generally involves the chemical reduction of gold salt in the aqueous, organic phase or in two phases [114]. However, the high surface energy of AuNPs makes them extremely reactive, and most systems undergo aggregation without protection or passivation of their surfaces [91, 114]. This way, special precautions have to be considered to avoid their aggregation and precipitation [114]. Typically the AuNPs synthesis is performed in the presence of a stabilizer which binds to their surface to impart high stability and high rich linking chemistry and provide the desired charge and solubility properties [91, 114].

The synthesis of AuNPs was reported firstly by Faraday in 1857 [117]. To date a large number of methods has already been developed to synthesize AuNPs. Among them, there are two classic ways which are widely employed. The first method for the

preparation of AuNPs in aqueous solution was introduced by Turkevich [120], which was subsequently improved by Frens [121]. In this method, AuNPs are prepared by reducing tetrachloroauric acid ($HAuCl_4$) with sodium citrate in boiling water (Turkevich-Frens method) [122]. The size of the synthesized AuNPs can range from 10-100 nm by changing the gold to citrate ratio [117]. The water soluble and negatively charged nanoparticles obtained via this method are usually utilized in the assembly of nano-composites and nano-interfaces based on electrostatic interactions [117, 118]. The second method was developed by Brust *et al.* in 1994 [123]. $AuCl_4^-$ was reduced by sodium borohydride in the presence of alkane thiols in a two phase system [118]. In addition to spherical nanoparticles, other Au structures can be generated in various shapes such as nanorods [124], nanoshells [125], nanocages [126] and nanocubes [127].

Compared to other nanomaterials, AuNPs are chemically stable, non-toxic and easy to functionalize. The stabilization and functionalization of AuNPs with biomolecular recognition motif have provided flexibility for a variety of applications, including bioassay, bioimaging and biosensor [115, 117, 118, 128]. As a result, DNA [129], enzymes [130], antibodies [131] and some functional polymers [132] can be easily conjugated with AuNPs without affecting their activities [118]. Different types of functionalized AuNPs can be developed as required [118].

From an electroanalytical point of view, AuNPs are particularly interesting because of their high stability, good biological compatibility, excellent conducting capability, and high surface-to-volume ratio [114, 119]. These features provide excellent prospects for interfacing biological recognition events with electronic signal transduction and make AuNPs extremely suitable for developing novel and improved electrochemical sensing and biosensing systems [91, 114, 117, 119]. They can be functionalized to detect specific targets, enabling the achievement of low detection limits, thus offering higher sensitivity and selectivity than conventional strategies. In addition, AuNPs present high conductivity essential for sensors based on electrical detection systems [91, 115, 116, 118, 119, 128].

Kang *et al*. [133] developed a sensitive immunosensor for Aβ42 using an electrical detection system based on scanning tunneling microscopy (STM). The immunosensor consisted on a sandwich immunoassay using an AuNPs-antibody conjugate. In this investigation, the authors concluded that β-amyloid could be successfully detected with electrical detection technique, achieving a 10 fg/mL detection limit. Georganopoulo *et al.* [134] used the bio-barcode system to detect

protein levels with attomolar sensitivity. The method involves the capture of the analyte with a magnetic particle featuring recognition elements, followed by binding of functionalized AuNPs with a second recognition agent and “barcode” (marker) DNA strands. After magnetic separation of the sandwich complex, the DNA barcodes are released and the DNA strands detected and quantified using the Au-nanoprobe sandwich assay followed by silver enhancement. This method was successfully used for measuring the concentration of amyloid-β-derived diffusible ligands, a potential Alzheimer’s disease marker present at extremely low concentrations (<1 pmol/L) in the cerebrospinal fluid of affected individuals [134].

Another relevant example includes the development of a novel enhancement for immunochromatographic test strips where both the primary and the secondary antibodies are conjugated with AuNPs [135]. This experimental set-up increased the detection limit of the chorionic gonadotropin hormone by an order of magnitude to reach 1 pg/mL.

3. Materials and Methods

3.1 Reagents and equipments

Alumina solution (γ-Al_2O_3) 0.3 µm and 0.05 µm were purchased from Gravimeta. All other reagents used were of analytical reagent grade. Sulfuric acid (H_2SO_4, 98%), hydrogen peroxide (H_2O_2, 30% Sigma-Aldrich, Steinheim, Germany) and absolute ethanol were purchased from Panreac (Spain). Potassium nitrate (KNO_3) was purchased from Pronalab (Mexico). Potassium ferrocyanide ($K_4[Fe(CN)_6].3H_2O$), potassium ferricyanide ($K_3Fe(CN)_6$), potassium hydrogen phosphate (K_2HPO_4) and potassium dihydrogen phosphate (KH_2PO_4) were purchased from Riedel-de Haën (Germany). N-(3, Dimethylaminopropyl)-N-ethyl-carbodiimide hydrochloride (EDC), 2-mercaptoethanol, 3-mercaptopropionic acid and glutaraldehyde solution were purchased from Fluka (Switzerland). N-hydroxysuccinimide (NHS), cystamine dihydrochloride, sodium citrate dihydrate, gold(III) chloride solution, ethylenediaminetetraacetic acid (EDTA), 2-imninothiolane hydrochloride, citrate buffer solution and 2,2′-Azino-bis(3-ethylbenzothiazoline-6-sulfonic acid) diammonium salt (ABTS) were purchased form Sigma-Aldrich (Steinheim, Germany). Milk powder was obtained from Molico Nestlé. Mouse monoclonal antibody to beta amyloid (1 mg/mL) IgG (ab11132) was purchased from Abcam (U.K). Human antigen β-amyloid peptide (1-42) was purchased from Genscript (USA). Goat anti-mouse IgG secondary antibody was purchased from Pierce antibodies/Thermo Scientific. Ultrapure water (18.2 $M\Omega cm^{-1}$ resistivity) was produced by a Milli-Q Simplicity 185 system (Millipore, Molsheim, France). Nitrogen (99.999%) was obtained from LINDE (Portugal).

The supporting electrolyte for the electrochemical studies was the phosphate buffer solution (0.1 mol/L, pH=7.4). A solution of 10 mmol/L $K_3[Fe(CN)_6]/K_4[Fe(CN)_6]$ was prepared in KNO_3 (1 mol/L).

pH measurements were performed using a pH meter (GLP 22, Crison) with a combined glass electrode.

Weight measurements were performed using an analytical balance (Mettler Toledo) with a 0.00001 g precision.

8 inches microcloth polishing cloth (Buehler) was used to perform the mechanical cleaning of the working electrode.

3.2 Electrochemical analyses

All voltammetric measurements were performed using Autolab electrochemical system (Eco Chemie, The Netherlands) equipped with PGSTAT-30 and General Purpose Electrochemical system for Windows (GPES) software (Figure 18). The electrochemical cell was assembled using a conventional three-electrode cell which included the developed biosensor (based on a polycrystalline gold electrode, BASi MF-2014, surface area 2.0 mm^2) as a working electrode, a glassy carbon as counter-electrode and a Ag|AgCl|KClsat reference electrode to which all potentials are referred (Figure 19).

All experiments were evaluated by square-wave voltammetry (SWV) and electrochemical impedance spectroscopy (EIS) using $Fe(CN)_6^{3-/4-}$ as electroactive indicator. SWV measurements were performed in a 0.1 mol/L PBS solution (pH=7.4) containing 0.01 mol/L of $K_3[Fe(CN)_6]/K_4[Fe(CN)_6]$ by varying the potential from 0.00 to 0.600 V at a 0.405 V/s scan rate. The optimal SWV parameters were a frequency of 100 Hz, amplitude of 40 mV and scan increment of 4 mV. EIS measurements were performed in a 0.01 mol/L $K_3[Fe(CN)_6]/K_4[Fe(CN)_6]$ solution using a frequency range from 10^{-1} to 10^5 Hz with an amplitude perturbation of 5 mV. Before the analysis, a 5 min nitrogen purge was performed.

Figure 18 – Potentiostat PGSTAT-30 (Autolab).

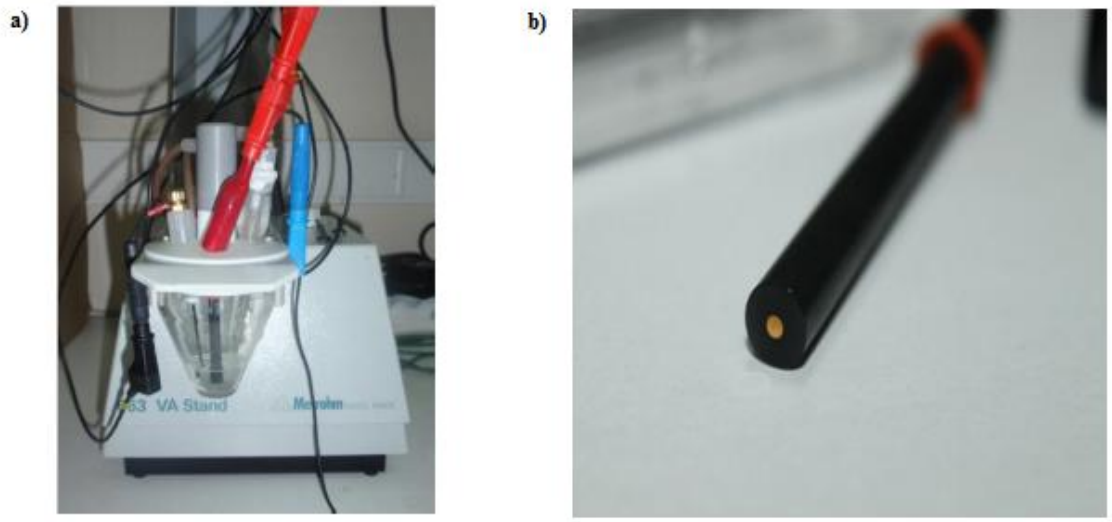

Figure 19 – a) Electrochemical cell assembly. Red: Working electrode; Black: Counter electrode; Blue: Reference electrode; b) Working electrode (gold electrode).

3.2.1 Pre-treatment of the working electrode

The pre-treatment of the gold electrode includes three stages: mechanical cleaning, chemical oxidation and electrochemical activation of the surface. The gold electrode was mechanically cleaned by polishing with γ-Al_2O_3 (0.3 μm and 0.05 μm) and then rinsed with water. Next, the gold electrode was immersed in piranha solution (H_2O_2:H_2SO_4, 1:3, v/v). For the electrochemical activation of the surface (to create –COOH and –OH functional groups onto the gold electrode), the electrode was cycled from 0.0 to +1.6 V in 0.5 mol/L H_2SO_4 solution at 100 mV/s. The electrochemical activation stage was also used to ensure the cleanliness of the gold electrode. The process was repeated until typical gold cyclic voltammograms were obtained.

3.2.2 Self-assembled monolayers

Several self-assembled monolayers (SAM) to modify the gold electrode surface were tested by immersing the gold electrode in 200 µL of the different SAM solutions for a 12 h period at room temperature: cystamine SAM 0.02 mol/L; cystamine and mercaptoethanol mixed SAM (100 µL cystamine 0.02 mol/L + 100 µL mercaptoethanol 0.02 mol/L); mercaptopropionic acid 1 mmol/L; mercaptopropionic acid and mercaptoethanol mixed SAM (100 µL mercaptopropionic acid 1 mmol/L + 100 µL mercaptoethanol 1 mmol/L). Ethanol was the utilized solvent to prepare the SAM solutions.

After washing with ultrapure water, the modified electrodes with cystamine were immersed in a 3% glutaraldehyde solution for 30 minutes. On the other hand, the modified electrodes with mercaptopropionic acid were immersed in a EDC/NHS solution (10 mg EDC + 10 mg NHS diluted in 500 µL PBS pH=7.4) for 30 minutes.

After selection of the appropriate SAM, the time of immersion and concentration of the solution for the SAM formation were optimized.

3.2.3 Synthesis and electrodeposition of gold nanoparticles

The gold nanoparticles (AuNPs) were synthesized by two different methods. In the first method AuNPs were synthesized in accordance with the Turkevich-Frens method by reduction of $HAuCl_4$ using sodium citrate [122]. Tetrachloroauric acid ($HAuCl_4$) aqueous solution (12.5 mL H_2O + 8.86 µL $HAuCl_4$) was warmed to slight boiling with continuously mechanical stirring. 1.25 mL of trisodium citrate 11.42 g/L were added and boiled for 15 min. The AuNPs solution was cooled at room temperature and stored at 4 ºC until further use. Hydrodynamic size and potential zeta values were characterized by dynamic light scattering and laser doppler velocimetry, respectively, using a Zetasizer Nano ZS (Malvern, UK), at 25ºC. AuNPs were also evaluated by UV/vis spectrophotometry (Shimadzu UV-1700 PharmaSpec spectrophotometer) at 527 nm. AuNPs electrodeposition on SAM modified gold electrode was carried out at -0.2 V for 600 s.

In the second method, the modified gold electrode was immersed in a 0.1 mol/L KNO_3 solution containing 3 mmol/L of $HAuCl_4$. AuNPs were synthesized during the electrochemical deposition by applying a -0.2 V potential for 200 s. Then the electrodeposition period was optimized.

3.2.4 Antibody immobilization

Antibody against β-amyloid was immobilized on the AuNPs using thiol (-SH) groups. In order to promote immobilization with the proper orientation the antibody was prepared through chemical modification (thiolation) with EDTA and iminothiolane. A mixed solution containing 1 µL of EDTA (0.28 mol/L), 82.6 µL of iminothiolane (0.198 mg/mL) and monoclonal antibody against Aβ42 was prepared after dilution with PBS; the volume of PBS added to the antibody was the necessary to make up a volume of 111 µL. The prepared solution reacted for 45 to 50 minutes at room temperature. After reaction 389 µL of PBS were added to the solution in order to make up a volume of 500 µL and the resulting solution was purified by passing it through a sephadex PD MiniTrap G-25 column (GE Healthcare), following the gravity protocol. In a first instant, the flow-through of the column was discarded. Then the column was eluted with 1.0 mL of PBS and the eluate was collected to an eppendorf. Three concentrations of antibody in PBS were tested (1.0 µg/mL, 2.5 µg/mL and 5.0 µg/mL). The SAM/AuNPs modified gold electrodes were immersed in 300 µL of the different antibody solutions, reacted for 2 h at room temperature and then were incubated at 4 ºC for 12 h. After concentration optimization, the incubation time was also optimized. For that purpose, five incubation times were tested 2.5, 5, 7.5, 10 and 12.5 h.

3.2.5 β-Amiloyd (1-42) detection

Firstly in order to evaluate the necessary time to promote the antibody-antigen reaction, an indirect ELISA assay was performed using ABTS as the detection product. The end product is green and the absorbance was measured at 405 nm. For the performance of the ELISA test the antigen was diluted in PBS (pH=7.4) to a final concentration of 90 µg/mL and the antigen was immobilized on the wells of a 96 well plate (Nunc MaxiSorp). The plate was then covered with an adhesive plastic and incubated at 37 ºC for 1 h. After the antigen immobilization it was necessary to block the remaining protein-binding sites in the coated wells by adding 10% non fat dry milk. The plate was covered with an adhesive plastic and incubated at 37 ºC for 1 h. Then diluted primary antibody was added to the coated wells and incubated at room temperature for 5 min. Next, the conjugated secondary antibody diluted in 3% non fat dry milk was added to the coated wells. At last, the substrate solution (ABTS) was

added and after sufficient colour development the optical density was measured at 405 nm. After each step the coated wells were washed three times with PBS.

After immobilization of the antibody and after washing with ultrapure water, the antibody/AuNPs/SAM modified gold electrodes were immersed in 300 μL of β-amyloid (1-42) solution for 5 min at room temperature. The antigen solutions were prepared in 0.1 mol/L PBS solution (pH=7.4). In this study eight antigen concentrations, 9028, 4514, 2257, 903, 451, 45.1, 4.51 and 0.451 ng/mL were used. The inhibition percentages (IR, %) and the selected antigen concentrations were employed to obtain the analytical data. The inhibition percentage (% IR) was calculated using the following equation (3):

$$\%IR=[1-(I_p/I_p^o)] \times 100 \quad (3)$$

where I_p^o and I_p are the peak currents before and after the incubation of the biosensor in the presence of the antigen solution.

The standard deviation of the intercepts and the average of slopes of the straight lines from the analytical curves were used to determine the detection (LOD) and quantification limits (LOQ) [136]. All measurements were made, at least, in duplicate.

4. Results and Discussion

4.1 Characterization of the electrode surface

The gold electrode (AuE) surface was qualitatively evaluated by cyclic voltammetry (Figure 20) in order to ensure that the surface was clean and appropriate to be modified in the subsequent experimental steps.

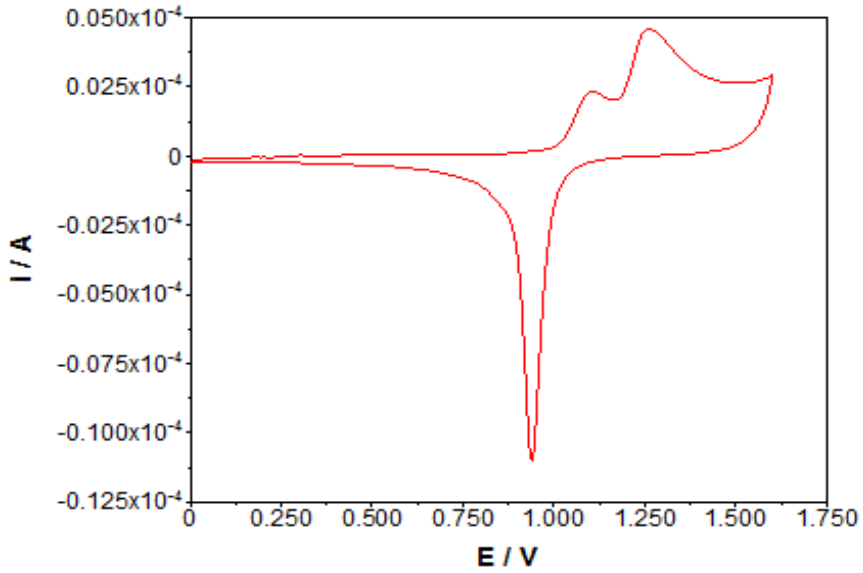

Figure 20 - Typical cyclic voltammogram obtained with a gold electrode in 0.5 mol/L H_2SO_4 aqueous solution at a 100 mV/s scan rate.

The characteristic voltammogram obtained (Figure 20) is in agreement with those found in literature [137]. In the first instants, the current is associated with charging of the double layer capacitance (Figure 7) [137]. Secondly, surface oxidation/reduction processes occur. Then in response to a change of potential with time, a faradaic current flows through the interface [137]. Surface processes are electrochemically limited by the quantity of a given material that can be deposited, reduced or changed at the gold interface, thereby giving rise to current peaks [137]. As observed in Figure 20, the voltammogram exhibited two broad oxidation peaks at 1.1 and 1.3 V, attributed to the formation of Au surface oxides, and a sharp reduction peak at 0.9 V due to subsequent removal of the oxides.

The profiles of cyclic voltammograms depend highly on the interface between the solution and the electrode. The state (chemical and physical) of the gold electrode is of vital importance in such experiments [137]. Also the electrolyte, chemicals, glassware, gas used to perform the purge of the solution, tubing for the gas, all have to be of high purity and extremely clean .

4.2 Biosensor construction

4.2.1 Modification of the AuE with self-assembled monolayers

Self-assembled monolayers (SAMs) have been used in electroanalytical chemistry for 30 years as the basis of electrochemical sensors [86]. SAMs are essentially organic assemblies that arrange themselves spontaneously at the solid-liquid interface induced by strong chemisorption between the substrate and the head group [87]. The main objective is the ability to modify and control the interface of certain materials by the assembling of individual molecules into highly ordered architectures, ensuring a homogeneous behavior of the surface, with a specific function.

Self-assembled monolayers offer several attractive features for applications in biosensors. First, since they use only the bare minimum resources, miniaturization is easy [87]. Secondly, the high degree of organization and dense nature of the SAMs chains mimic the cellular microenvironment of lipid bilayer structures providing novel substrates for the immobilization of biomolecules or biological systems [87]. In addition, the ability to select the functional groups of the monolayers allows better control of the nanoarchitecture, enabling the attachment of nanoclusters of either metals or semiconductors [87]. One of the most important advantages of SAMs consists on its easy preparation. The substrate just has to be immersed in a dilute solution of the adsorbate at a selected temperature for a specific period of time. Moreover compatibility with metal substrates (Au, Ag, etc.) for electrochemical measurements enables special benefits for biosensor applications involving current or potential measurements [87]. At last, the chemical stability presented by these monolayers even after the coupling with biomolecules for biological sensing makes them suitable to work as biosensor and immunosensors [87]. This way, SAMs composed of thiols or dithiols on metals, particularly on gold, have been the focus of considerable attention due to the fact of combining the mentioned characteristics, especially the ease of preparation and the high stability attained from the S-Au bond and by van der Walls interactions [82, 86, 87].

Several factors affect the formation and packing density of monolayers like the nature and roughness of substrate, solvent, nature and concentration of the adsorbate, and the temperature [87]. Cleanliness and crystallinity of the substrate also play a crucial role in determining the compactness of the SAM [87]. These facts highlight the importance of the pre-treatment stage and the SAM formation should be performed immediately after this step. The time of immersion of the substrate in the solution also

plays an important role in the SAM formation and usually high concentrations require low immersion periods.

In this work four different SAMs to modify the gold electrode surface were studied and as mentioned previously the redox pair $Fe(CN)_6^{3-/4-}$ was used to study the electrochemical behaviour of the gold electrode before and after the depositions. The modification of the gold electrode with the SAMs led to a block in the electron transfer between the surface of the electrode and the solution which consequently caused a large signal reduction, as it can be observed in Figure 21. This fact shows that the adsorption of the SAMs on the gold electrode surface was successful. The SAMs that best adsorbed to the electrode surface were the ones that caused the largest signal reduction. From observation of Figure 21, it can be concluded that the SAMs composed of mercaptopropionic acid, cystamine and mercaptopropionic acid+mercaptoethanol achieved better adsorptions. On the other hand cystamine+mercaptethanol mixed SAM adsorbed in a lesser extend onto the gold surface as the signal reduction was not so large when compared to the other SAMs.

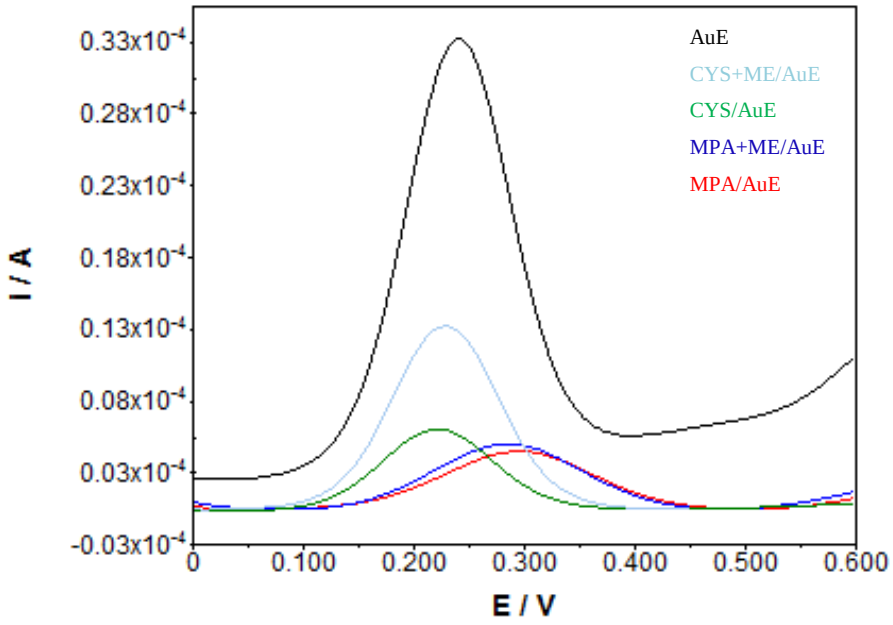

Figure 21 - Comparison of the different square-wave voltammograms before (AuE) and after the modification with the different self-assembled monolayers (12 h immersion): cystamine SAM (CYS); cystamine and mercaptoethanol mixed SAM (CYS+ME); mercaptopropionic acid SAM (MPA); mercaptopropionic acid and mercaptoethanol mixed SAM (MPA+ME). Profiles obtained in a 0.1 mol/L PBS solution pH=7.4 containing 0.01 mol/L $Fe(CN)_6^{3-/4-}$ at a 0.405 V/s scan rate.

The SAMs functional groups were properly activated. In the case of cystamine SAMs, the amina group ($-NH_2$) was activated by a glutaraldehyde solution, and the

carboxylic (-COOH) group of the mercaptopropionic acid SAMs was activated by an EDC/NHS solution enabling future anchoring of proteins or nanomaterials.

At this stage the objective was to choose the most appropriate SAM to modify the gold electrode. That way, mercaptopropionic acid SAM was the selected one as it presented the largest signal reduction.

The most common protocol for preparing SAMs on gold is immersion of the clean substrate into a dilute ethanolic (1~10 mmol/L) solution for ~12-18 h at room temperature [84]. In order to optimize the biosensor construction, shorter immersion times for the selected mercaptopropionic acid SAM (1 mmol/L) were tested in this work. From Figure 22 it can be concluded that a 2 h immersion time was enough to promote the formation of the mercaptopropionic acid SAM on the gold surface.

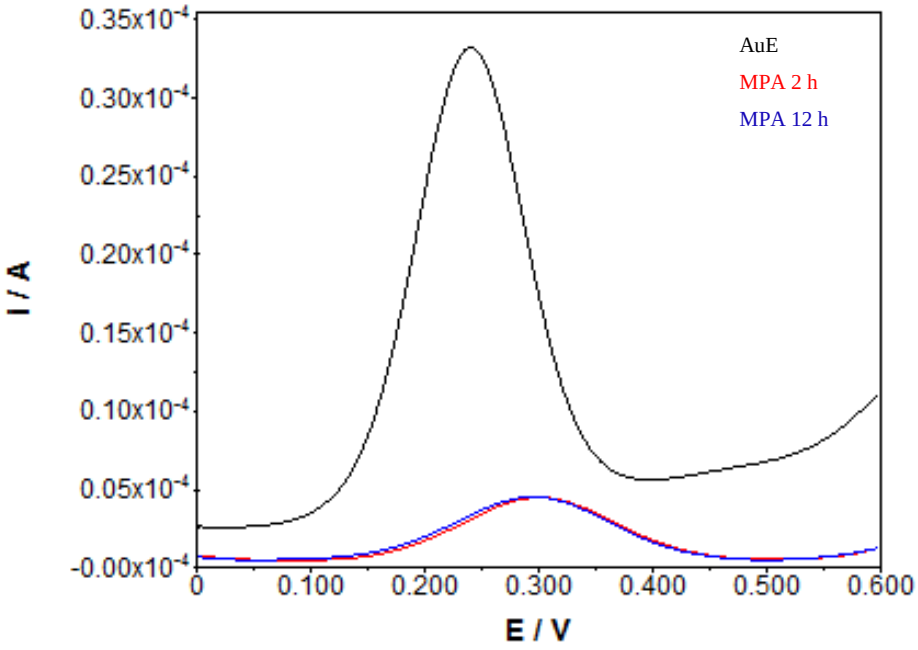

Figure 22 – Square-wave voltammograms obtained for different immersion periods of the gold electrode (AuE) on the 1 mmol/L mercaptopropionic acid solution. Profiles obtained in a 0.1 mol/L PBS solution pH=7.4 containing 0.01 mol/L $Fe(CN)_6^{3-/4-}$ at a 0.405 V/s scan rate.

Applying the optimum immersion time, the concentration of the mercaptopropionic acid solution was also optimized. Five concentrations ranging from 1 to 20 mmol/L were studied. As it can be observed in Figure 23, the appropriate concentration to promote the formation of the SAM for a 2 h period was 5 mmol/L as it attained the more stable, largest and reproducible signal reduction.

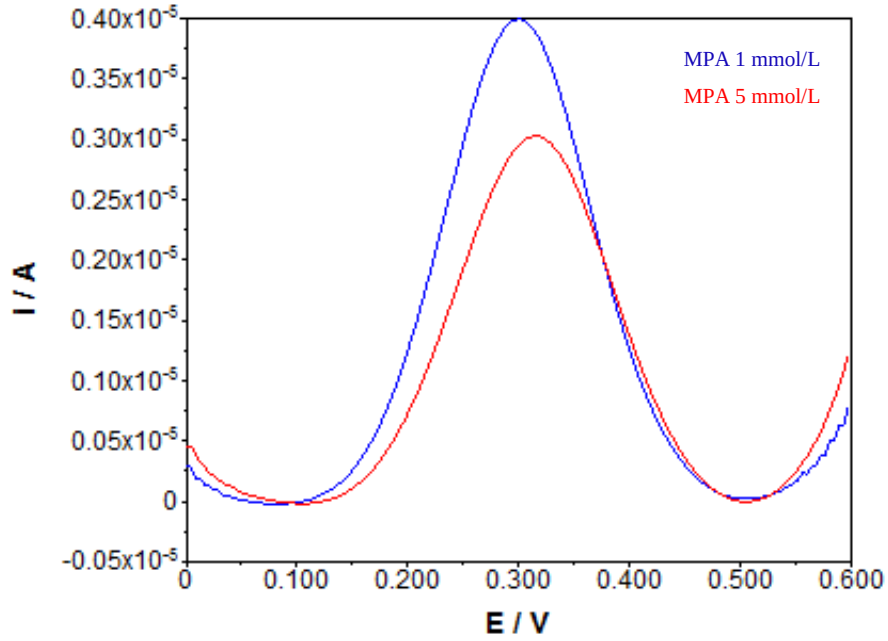

Figure 23 - Square-wave voltammograms obtained for different concentrations of MPA solution for a 2 h immersion period. Profiles obtained in a 0.1 mol/L PBS solution pH=7.4 containing 0.01 mol/L $Fe(CN)_6^{3-/4-}$ at a 0.405 V/s scan rate.

Figure 24 shows the impedance spectra recorded for the gold electrode before and after the SAM formation. The diameter of the semicircle in the Nyquist plot, which indicated the electron transfer resistance of the layer, can be used to describe the interface properties of the electrode for each modification step. The immobilization of the mercaptopropionic acid SAM led to a significant change in the impedance spectra when compared to the bare gold electrode which showed a straight line characteristic of a diffusion limit process. The MPA SAM formation on the gold electrode surface induced an increase in diameter of the semicircle component of the Nyquist plot which reflects the formation of an organized and packed layer that increases the charge-transfer resistance.

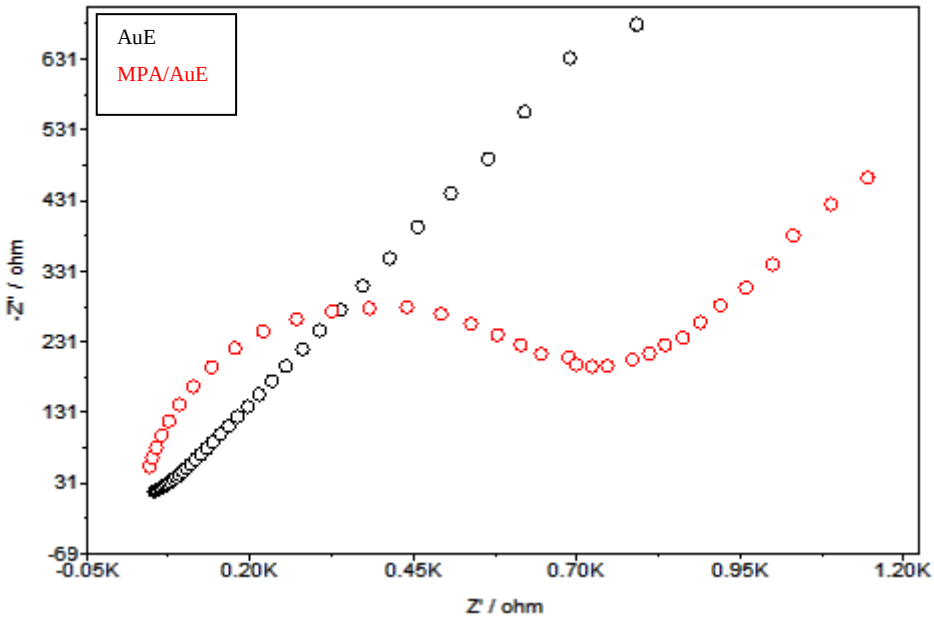

Figure 24 - Nyquist plot of electrochemical impedance spectra for bare gold electrode (AuE) and MPA SAM modified gold electrode. Profiles obtained in a 0.01 mol/L $Fe(CN)_6^{3-/4-}$ solution by applying a frequency range from 10^{-1} to 10^5 Hz with an amplitude perturbation of 5 mV.

4.2.2 Deposition of gold nanoparticles onto the MPA/AuE

In recent years, the field of electrochemical biosensors design has been capable of providing better analytical characteristics in terms of sensitivity, selectivity reliability, ease of use and low cost. As a kind of novel material, nanoparticles show new strategies to enhance signal response and may help developing novel sensors for biomedical applications [119, 128]. Nanosized particles of noble metals have been the source of particular interest due to their distinct physical and chemical properties. The catalytic capacity of metal nanoparticles to amplify the electrochemical reactions gives them a significantly priority in the construction of electrochemical biosensors.

AuNPs can promote the link between the redox centers in proteins and electrode surfaces due to their excellent conductivity and catalytic properties [138]. AuNPs are highly stable and less vulnerable to degradation caused by the solution matrix [138]. Moreover, AuNPs are non-toxic, easy to functionalize, biocompatible to both *in vivo* and *in vitro* environments and present a large surface area to volume ratio. That way, AuNPs provide a great interface for biological recognition and electronic transduction which make them become an essential part in bioelectrochemistry [118]. Therefore AuNPs are employed as substrate to immobilize proteins or enzymes to provide a

suitable microenvironment on the electrode and lend more freedom of orientation to enhance the direct electron transfer behavior [55].

In this work two methods were used to synthesize the AuNPs. Firstly, the AuNPs were synthesized by the Turkevich-Frens method [122]. As mentioned previously, in this method AuNPs were prepared by reducing tetrachloroauric acid ($HAuCl_4$) with sodium citrate in boiling water. Produced nanoparticles were spectrophotometrically characterized in a range of 200 to 700 nm (Figure 25). From wavelength analysis of the predominant detected peak, the AuNPs size may be estimated in accordance with Link *et al.* [139]. That way, from observation of Figure 25 it is possible to conclude that the nanoparticles solution exhibits an absorbance peak at 527 nm which correspond to a diameter of 30 ± 10 nm [139]. This data is in accordance with the AuNPs characterization performed by dynamic light scattering. From these measurements it was concluded that the nanoparticles presented a hydrodynamic size of 36.8 ± 0.57 nm. The potential zeta of the AuNPs was -38.1 ± 2.1 mV, confirming the stability of the nanoparticles attained by the citrate-capped effect.

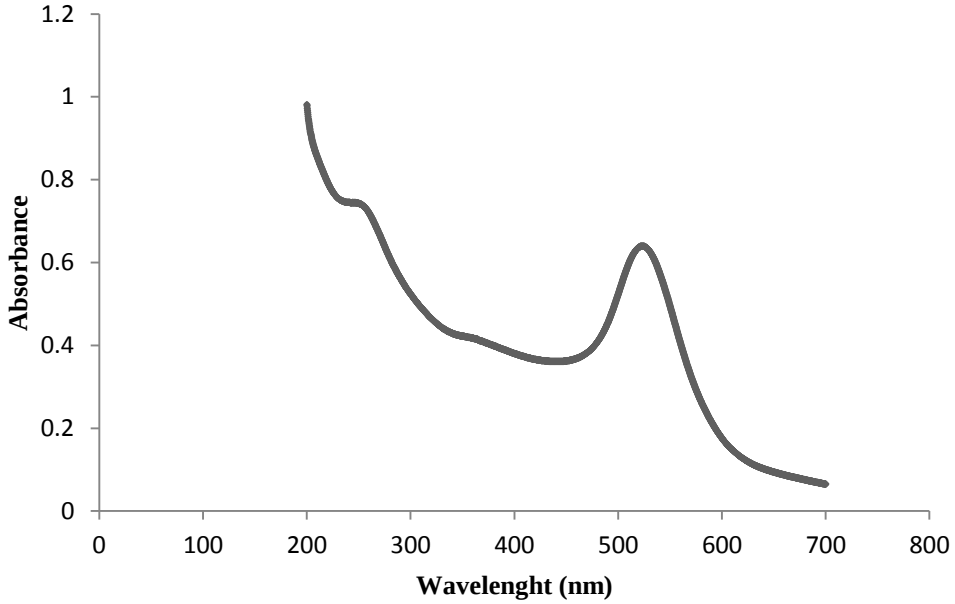

Figure 25 - Absorption spectrum of the gold nanoparticles prepared by the Turkevich-Frens method.

The immobilization of AuNPs onto the MPA/AuE is usually performed by two methods: electrodeposition or/and by covalent and electrostatic interactions with self-assembled monolayers that present the appropriate functional groups for that purpose.

In this work the nanoparticles were immobilized on the mercaptopropionic acid SAM by electrodeposition, which consists in the application of -0.2 V for 600 s.

The second method tested for the AuNPs synthesis is based on the electrodeposition process that occurs at -0.2 V for 200 s when the MPA/AuE is immersed in a KNO_3 solution containing $HAuCl_4$ [140]. The AuNPs deposition on the MPA/AuE led to a significantly signal enhancement of the $Fe(CN)_6^{3-/4-}$ redox pair (Figure 26) associated with the increase of the gold electrode area and conductivity.

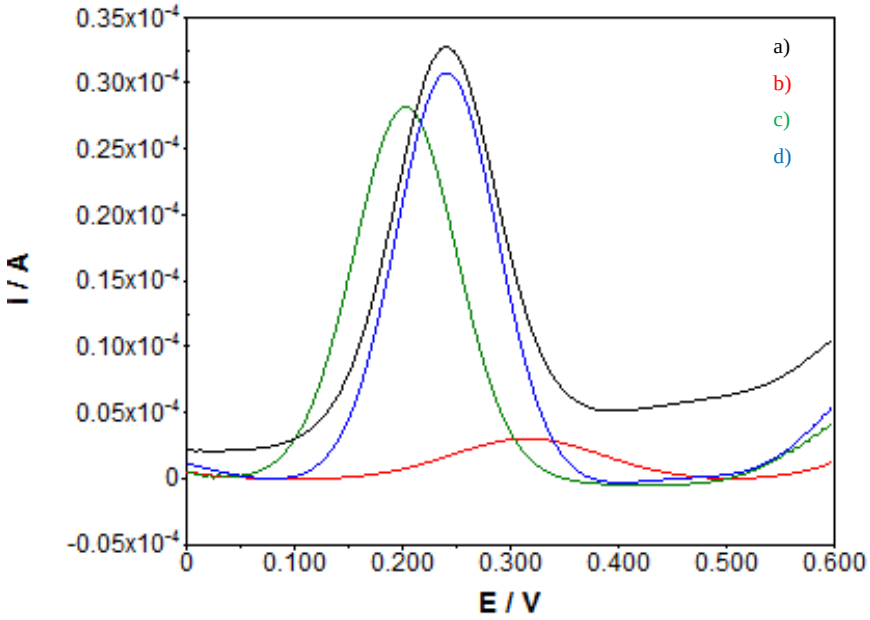

Figure 26 - Square-wave voltammograms obtained for the bare gold electrode (a), after modification with the 5 mmol/L MPA SAM (b), and electrodeposition of AuNPs synthesized by the Turkevich-Frens method during 600 s (c) and by the potential application during 200 s (d). Profiles obtained in a 0.1 mol/L PBS solution pH=7.4 containing 0.01 mol/L $Fe(CN)_6^{3-/4-}$ at a 0.405 V/s scan rate.

From Figure 26 it can be concluded that the AuNPs synthesized by the both methods caused approximately the same signal enhancement when deposition is applied during 600 and 200 s, respectively for the AuNPs produced by the Turkevich-Frens method and by electrodeposition. Consequently, this second procedure was chosen to obtain the AuNPs/MPA/AuE biosensor since it constitutes a simpler and faster process.

The results of the optimization of AuNPs electrodeposition time are presented in Figure 27. It can be concluded that a 100 s period is sufficient to promote a successful synthesis and deposition of AuNPs since the three tested period of time promoted almost the same signal enhancement.

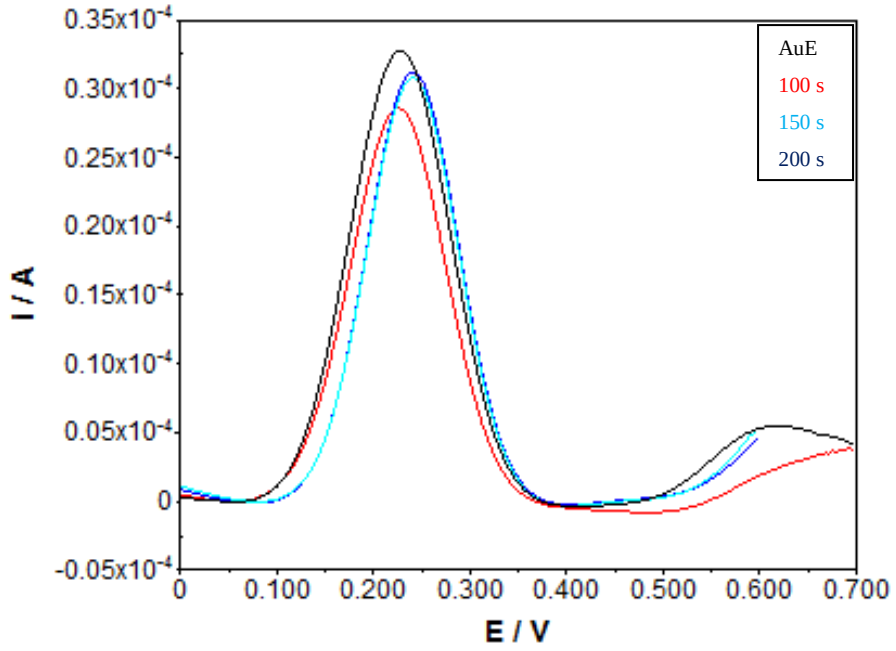

Figure 27 – Square-wave voltammograms obtained with the bare gold electrode (AuE) and AuNPs/MPA/AuE biosensor for different AuNPs electrodeposition periods. Profiles obtained in a 0.1 mol/L PBS solution pH=7.4 containing 0.01 mol/L $Fe(CN)_6^{3-/4-}$ at a 0.405 V/s scan rate.

EIS was also applied since it is an effective tool for the characterization of the interface properties of the electrode surface during different modification steps. The obtained Nyquist diagrams at the bare AuE, MPA/AuE and AuNPs/MPA/AuE sensor are exhibited in Figure 28. At high frequencies, the diameter of the semicircular portion controls the electron transfer kinetics of the redox process at the electrode interface. It dramatically decreased after modification of the MPA/AuE with AuNPs. In the presence of AuNPs the system exhibited a better performance as electrochemical biosensor. AuNPs are widely used nanomaterials because of their large surface area, strong adsorption ability, and high conductivity [114, 115, 118]. Their conductivity characteristics improve the electron transfer at the electrode surface. They can strongly interact with biomaterials and they have been used as a mediator to immobilize biomolecules and to efficiently retain their activity. Thus they will enable the immobilization of the antibody. At lower frequencies, the linear part is typical of a mass diffusion-limited electron-transfer process.

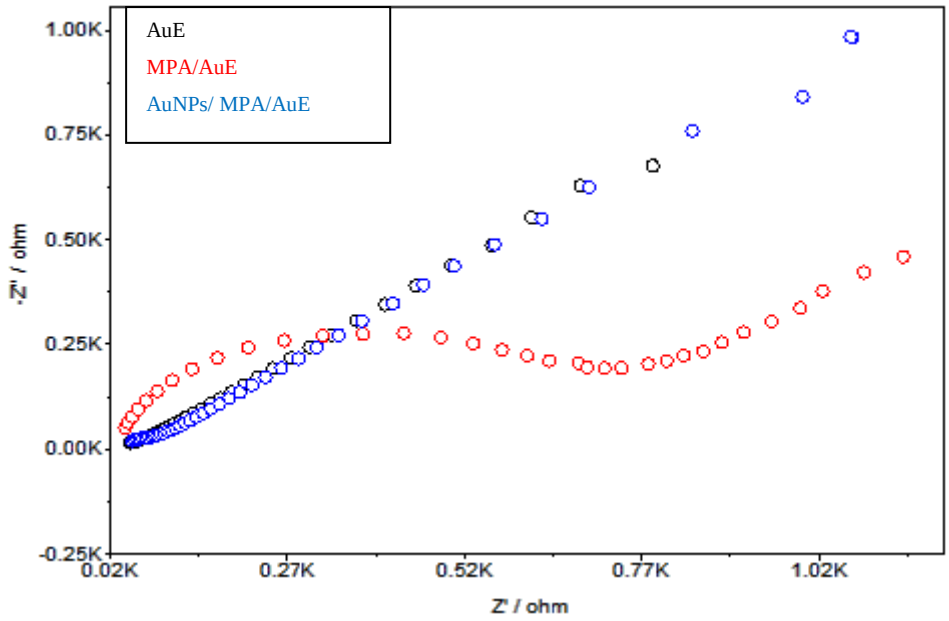

Figure 28 - Nyquist plot of electrochemical impedance spectra for bare gold electrode (AuE), MPA/AuE and AuNPs/MPA/AuE. Profiles obtained in a 0.01 mol/L $Fe(CN)_6^{3-/4-}$ solution by applying a frequency range from 10^{-1} to 10^5 Hz with an amplitude perturbation of 5 mV.

4.2.3 Antibody immobilization onto the AuNPs/MPA/AuE

The antibodies were functionalized through chemical modification (thiolation) to promote the antibody immobilization with the proper orientation. The objective of this treatment was to encourage the antibody immobilization to the AuNPs using thiol groups created in the Fc section of the antibody (Figure 12) in order to make the antigen binding site available. For this purpose the antibody was treated with Traut's reagent, or 2-iminothiolane, and EDTA. The reagent reacted with the amine groups in the antibodies to result in permanent modifications containing terminal sulfhydryl residues [141]. EDTA was required to stop completely metal-catalyzed oxidation of sulfhydryl groups [141]. Three concentrations (1.0, 2.5 and 5.0 µg/mL) of antibody were tested and a large signal reduction for the $Fe(CN)_6^{3-/4-}$ redox couple was observed (Figure 29). This peak diminution is caused by the partial blockage of the AuNPs/MPA/AuE surface by the antibodies making the electron transfer process between the electrode and the solution slower and more difficult. The spectra attained by EIS (Figure 30) also supported these results confirming that the antibody was successfully immobilized at the AuNPs/MPA/AuE surface. The semicircle diameter at high frequencies was significantly enlarged after immobilization of the antibody and the enlargement of the semicircle diameter seemed proportional to the antibody concentration.

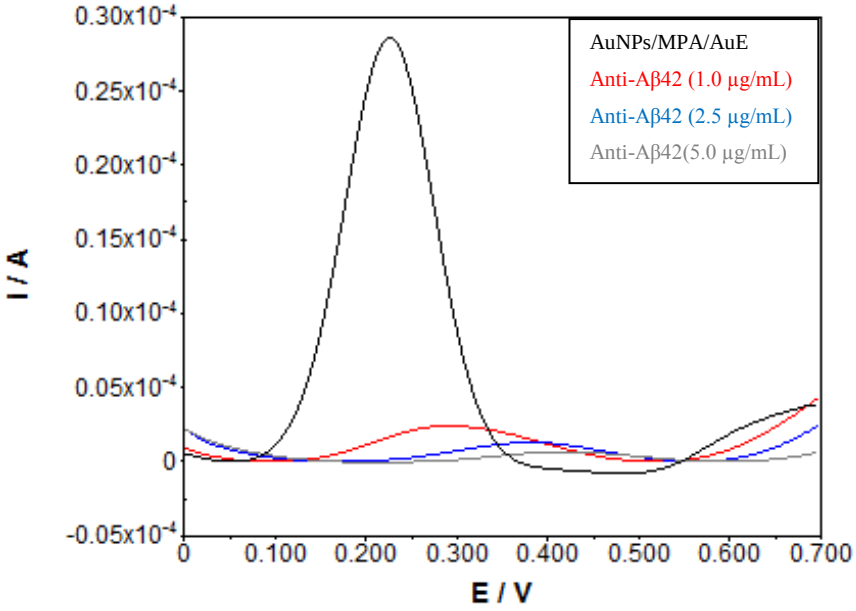

Figure 29 – Square-wave voltammograms obtained for AuNPs/MPA/AuE and AuNPs/MPA/AuE modified with different antibody concentrations for a 12 h incubation time. Profiles obtained in a 0.1 mol/L PBS solution pH=7.4 containing 0.01 mol/L $Fe(CN)_6^{3-/4-}$ at a 0.405 V/s scan rate.

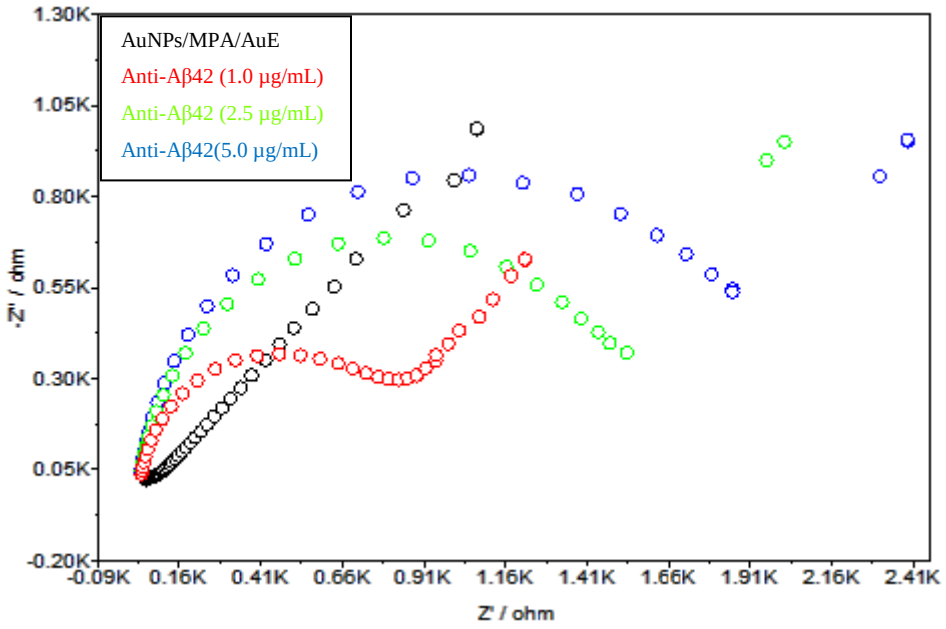

Figure 30 - Nyquist plot of electrochemical impedance spectra for AuNPs/MPA/AuE and AuNPs/MPA/AuE modified with different antibody concentrations. Profiles obtained in a 0.01 mol/L $Fe(CN)_6^{3-/4-}$ solution by applying a frequency range from 10^{-1} to 10^5 Hz with an amplitude perturbation of 5 mV.

The concentration that seems to best suit the objective of the work was the amount of 1.0 µg/mL because a high or complete blockage of the surface is undesirable since it would difficult or preclude the antigen quantification. Despite the lower signal reduction achieved with the concentration 1.0 µg/mL, an optimization of the incubation time was performed in order to accomplish a successful immobilization of the antibodies that enabled at the same time the quantification of Aβ42. Five incubation times (2.5, 5, 7.5, 10 and 12.5 h) were tested and the results achieved are exhibited in Figure 31. The 7.5 h incubation time was selected as the most adequate since the signal was reduced to approximately half of the one obtained with AuNPs/MPA/AuE. It ensures the successful antibody immobilization and still enables future antigen quantification. The lower incubation times (2.5 and 5 h) caused a slight signal reduction which did not assure a good antibody immobilization. On the other hand, the highest incubation times (10 and 12.5 h) caused a large signal reduction which would not allow the antigen quantification to be performed.

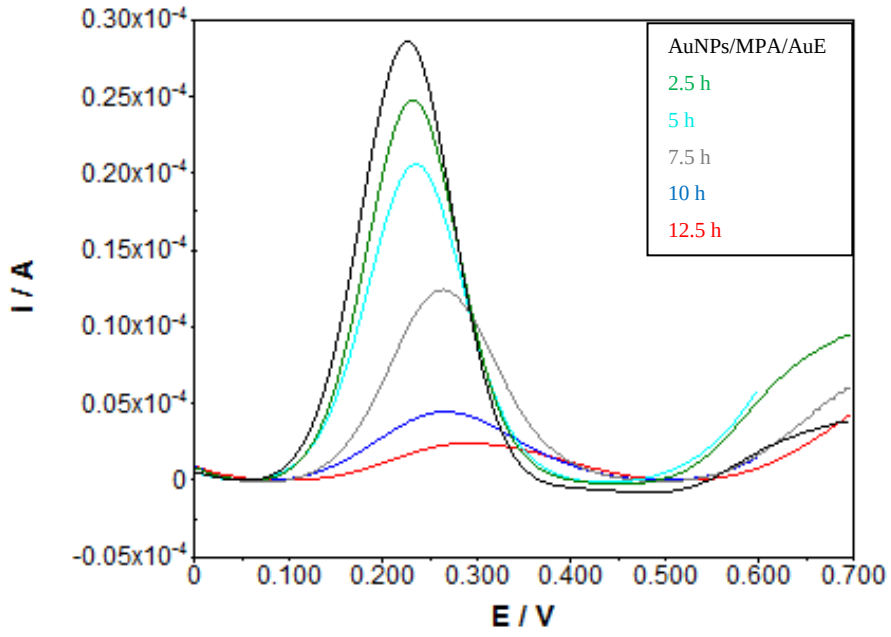

Figure 31 - Square-wave voltammograms obtained with the AuNPs/MPA/AuE and the AuNPs/MPA/AuE modified with different antibody (1.0 µg/mL) incubation times. Profiles obtained in a 0.1 mol/L PBS solution pH=7.4 containing 0.01 mol/L $Fe(CN)_6^{3-/4-}$ at a 0.405 V/s scan rate.

The impedance spectra attained with the AuNPs/MPA/AuE modified with different antibody (1.0 µg/mL) incubation times are presented in Figure 32. The results are in agreement with those obtained by square-wave voltammetry. The diameter of the

semicircles was proportional to the incubation times. In the case of higher incubation times it was observed an increase in the electron transfer resistance which corresponds to the immobilization of higher amounts of antibodies on the biosensor. On the other hand lower incubation times exhibited small diameters which exalts the immobilization of small amounts of antibodies facilitating the electron transfer process between the modified gold electrode and $Fe(CN)_6^{3-/4-}$. Figure 33 summarizes the results of impedance spectroscopy concerning the biosensor construction.

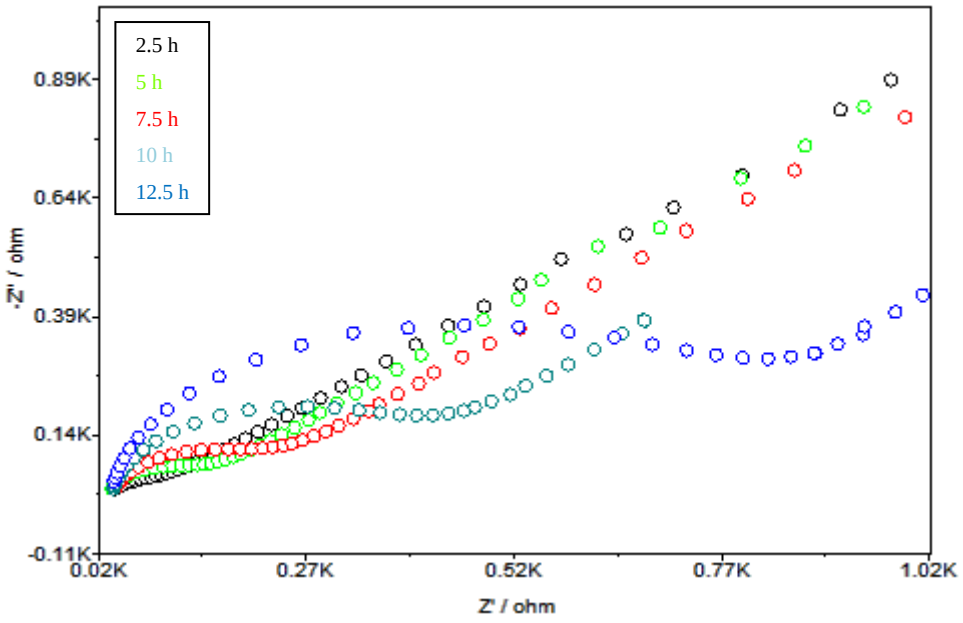

Figure 32 - Nyquist plot of electrochemical impedance spectra for the AuNPs/MPA/AuE modified with different antibody (1.0 µg/mL) incubation times. Profiles obtained in a 0.01 mol/L $Fe(CN)_6^{3-/4-}$ solution by applying a frequency range from 10^{-1} to 10^5 Hz with an amplitude perturbation of 5 mV.

The next step after antibody immobilization usually is the immobilization of bovine serum albumin (BSA) in order to minimize the nonspecific binding of interfering species present in samples such as serum and blood [68]. However as this sensor was only studied in PBS solutions containing Aβ42 the risk of occurring nonspecific bindings was abolished. Nevertheless, it is important to refer that this is an important step and it is going to be implemented before future tests in samples such as serum, blood or cerebrospinal fluid.

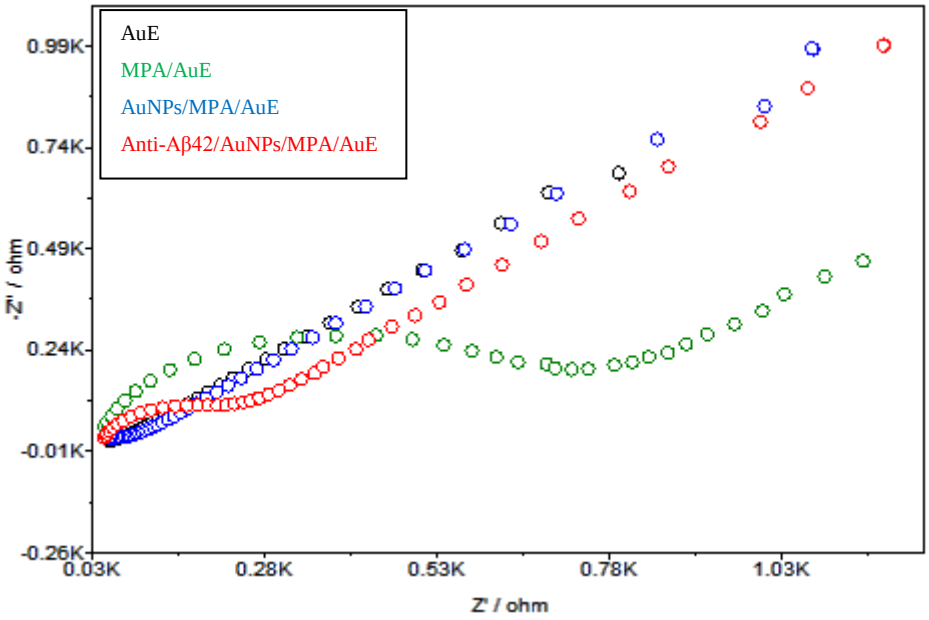

Figure 33 - Nyquist plot of electrochemical impedance spectra for the AuE, MPA/AuE, AuNPs/MPA/AuE and Anti-Aβ42/AuNPs/MPA/AuE. Profiles obtained in a 0.01 mol/L $Fe(CN)_6^{3-/4-}$ solution by applying a frequency range from 10^{-1} to 10^5 Hz with an amplitude perturbation of 5 mV.

4.3 Amyloid β (1-42) detection

In order to evaluate the necessary time to promote the antibody-antigen reaction, an indirect ELISA assay performed at 405 nm using ABTS as the detection product was performed. The final product is green making easy to detect the development of the reaction. As a result of this test it was concluded that a 5 min period was enough to promote the link between the antigen and the antibody.

Square-wave voltammetry was used to analyze Aβ42 concentrations based on the current intensity I_p^o and I_p measured before and after the incubation of the immunosensor in the presence of the antigen solution. The antibody-antigen interaction led to a signal reduction caused by the blockage of the surface making the electron transfer process between the Anti-Aβ42/AuNPs/MPA/AuE surface and $Fe(CN)_6^{3-/4-}$ more difficult. The decrease of the peak current intensities is proportional to the increase of the Aβ42 concentration (0-9028 ng/mL) (Figure 34). These results of SWV and EIS (Figure 35) indicate that the binding of the Aβ42 antigen to the Aβ42 antibody further blocks the electrode transfer barrier and increases the electron transfer resistance in electrochemical impedance measurements.

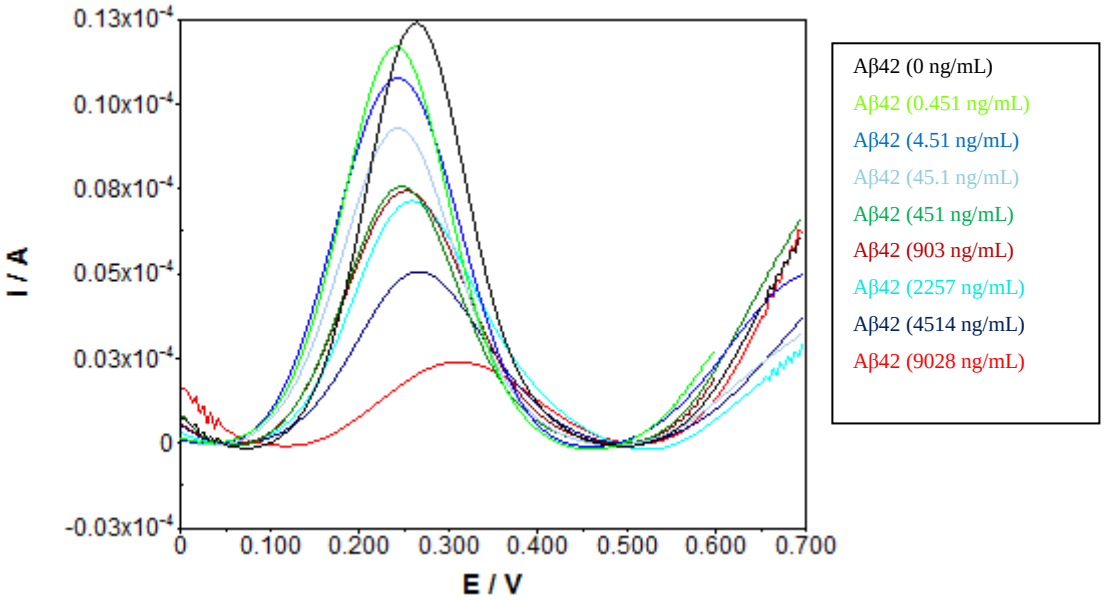

Figure 34 - Square-wave voltammograms obtained with the Anti-Aβ42/AuNPs/MPA/AuE immunosensor after expositions to different Aβ42 concentrations (0 to 9028 ng/mL). Profiles obtained in a 0.1 mol/L PBS solution pH=7.4 containing 0.01 mol/L $Fe(CN)_6^{3-/4-}$ at a 0.405 V/s scan rate.

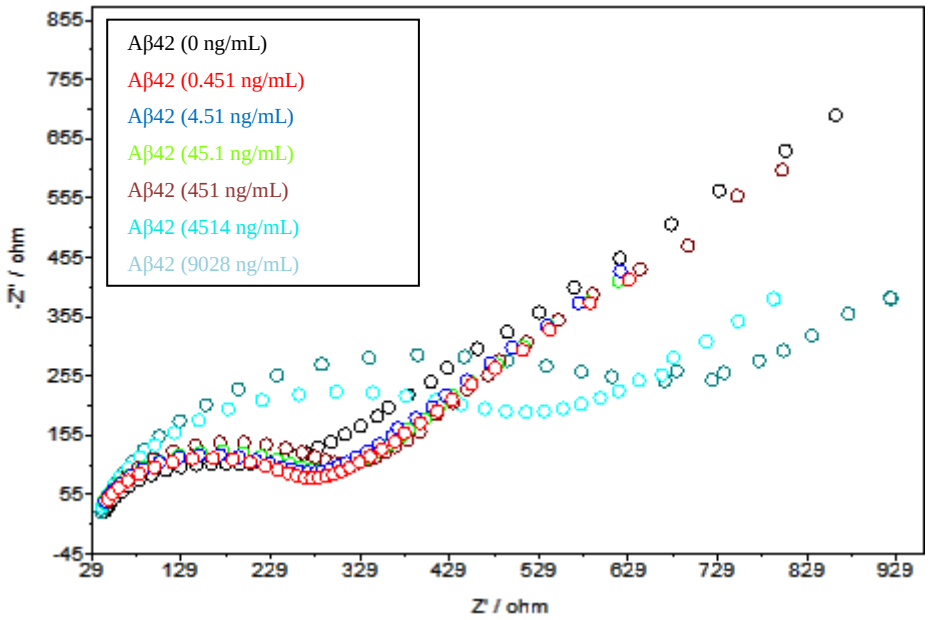

Figure 35 - Nyquist plot of electrochemical impedance spectra observed with the Anti-Aβ42/AuNPs/MPA/AuE immunosensor after expositions to different Aβ42 concentrations (0 to 9028 ng/mL). Profiles obtained in a 0.01 mol/L $Fe(CN)_6^{3-/4-}$ solution by applying a frequency range from 10^{-1} to 10^5 Hz with an amplitude perturbation of 5 mV.

Figure 36 shows the several stages for the biosensor construction. Figure 37 shows the same process but in an impedance spectra reached in a solution of 0.01 mol/L of $Fe(CN)_6^{3-/4-}$. The diameter of the semicircle in the Nyquist plot, which exhibits the electron transfer resistance of the layer, can be used to describe the interface properties

of the electrode for each immobilized step. Firstly, the bare gold electrode exhibited a straight line characteristic of the diffusion limit process. Secondly, the mercaptopropionic acid SAM was immobilized on the gold electrode, blocking its surface and increasing the electron transfer resistance leading to an enlargement of the semicircle diameter. Then AuNPs were electrodeposited onto the MPA/AuE decreasing significantly the electron transfer resistance and consequently the semicircle diameter was reduced to an almost straight line. In the next step AuNPs/MPA/AuE was immersed in the antibody solution (1.0 µg/mL) for 7.5 h and the immobilized antibody hindered the electron transfer process increasing again the diameter of the semicircle. At last, the Anti-Aβ42/AuNPs/MPA/AuE was immersed for 5 minutes in an antigen solution causing an even higher blockage of the surface, leading to the increase of the electron transfer resistance and consequently an increase of the semicircle diameter.

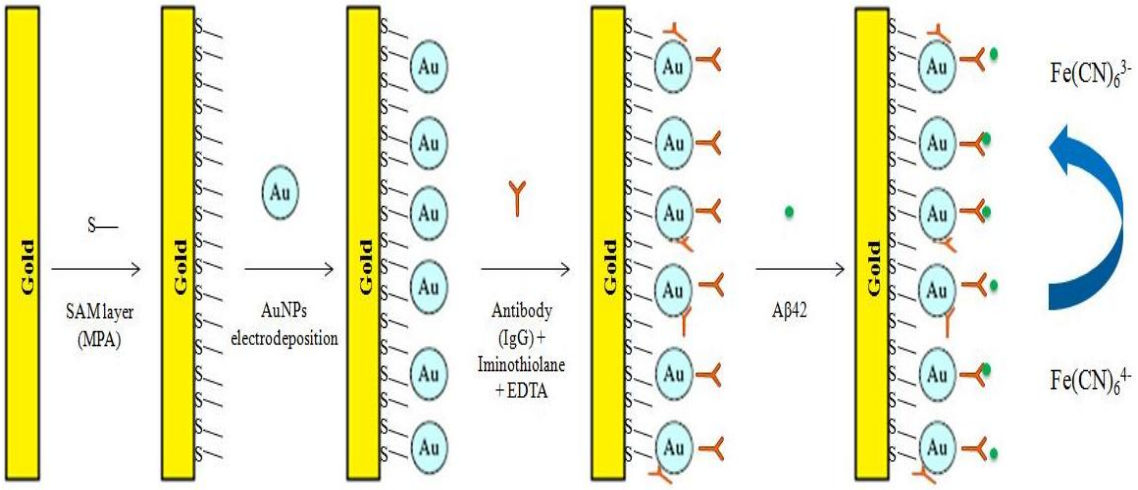

Figure 36 - The several steps for the biosensor construction.

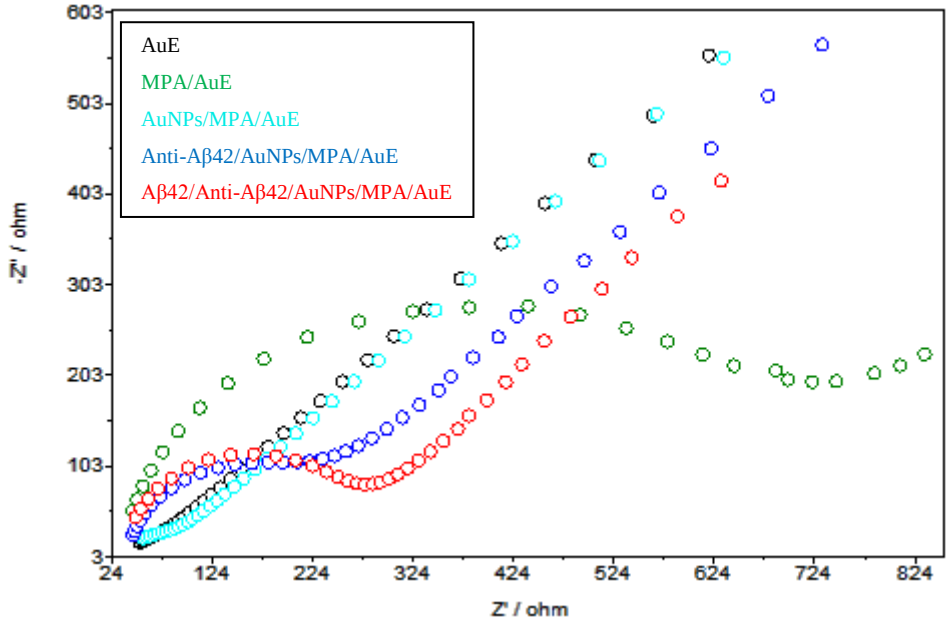

Figure 37 - Nyquist plot of electrochemical impedance spectra for the different stages of the immunosensor construction. Profiles obtained in a 0.01 mol/L $Fe(CN)_6^{3-/4-}$ solution by applying a frequency range from 10^{-1} to 10^5 Hz with an amplitude perturbation of 5 mV.

Applying the optimized square-wave voltammetric parameters (frequency 100 Hz, pulse amplitude 40 mV and scan increment 4 mV), calibration data were attained for Aβ42 concentrations ranging from 0.451 to 9028 ng/mL using two constructed biosensors (Figures 38-39). The analytical curve presented a wide concentration range (0.451 to 2257 ng/mL), linearity and low dispersion of the data, even at low concentrations, with high quadratic correlation coefficients of 0.998. The reduction of the peak current (%) depends linearly on the logarithm of Aβ42 concentration (Figure 39). The detection limit was found to be 264 pg/mL (58 pmol/L). This value is lower than the previously reported ones for the detection of Aβ42 based on electrochemical principles [142-145]. Vestergaard *et al.* [142] developed a rapid label-free electrochemical detection based on cyclic and square-wave voltammetry techniques for Alzheimer's Aβ aggregation based on the study of tyrosine oxidation achieving a detection limit of approximately 0.7 μg/mL for Aβ40 and Aβ42. Prabhulkar *et al.* [143] developed a microbiosensor using a triple barrel carbon fiber microelectrode as the sensor platform. Square-wave voltammetry was used to measure the intrinsic oxidation signal of Aβ originated from a single tyrosine residue. This biosensor was applied to detection of Aβ40 and Aβ42 in mice CSF within a detection range of 20-50 nmol/L and 20-140 nmol/L, respectively. Li *et al.* [144] developed an electrochemical biosensor using SWV for the detection of Aβ42 soluble oligomer. The peptide was immobilized in a mercaptoundecanoic acid SAM and levels as low as 240 pmol/L were detected.

Chikae *et al.* [145] developed a sensor for Aβ detection with saccharide immobilized gold nanoparticles on carbon electrode. The detection of Aβ was performed by the electrochemical sensing of saccharide-protein interactions. This developed sensor had a detection limit of 1 µmol/L for Aβ40 and Aβ42.

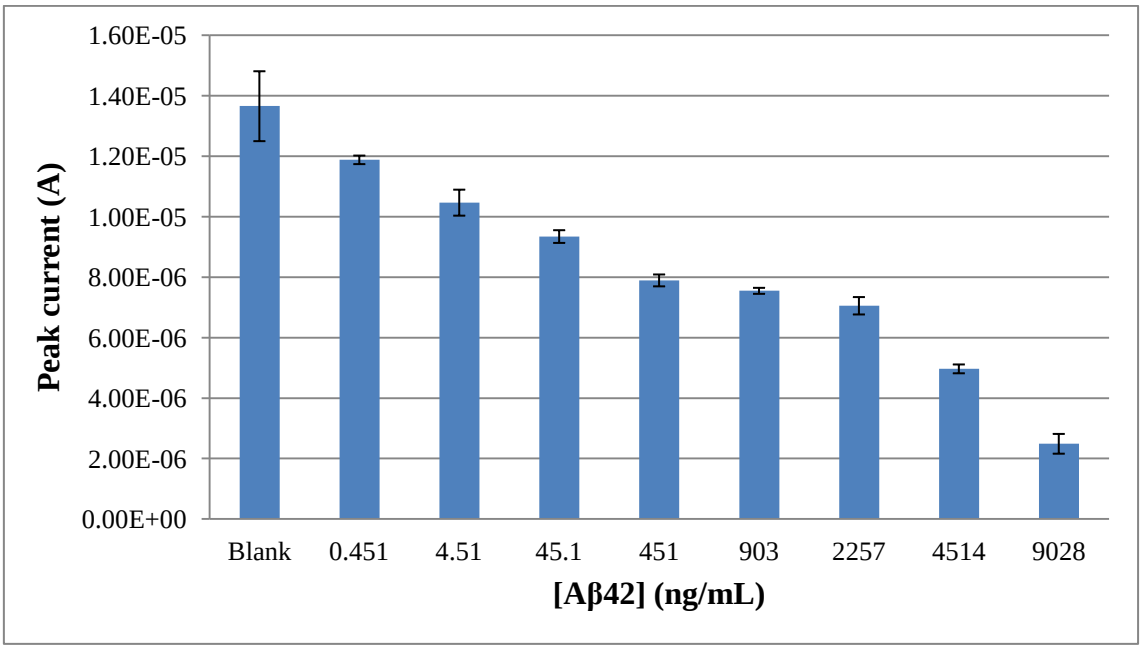

Figure 38 - Effect of the Aβ42 concentration (ng/mL) on the peak current (A) of the immunosensor. Error bars correspond to three replicates.

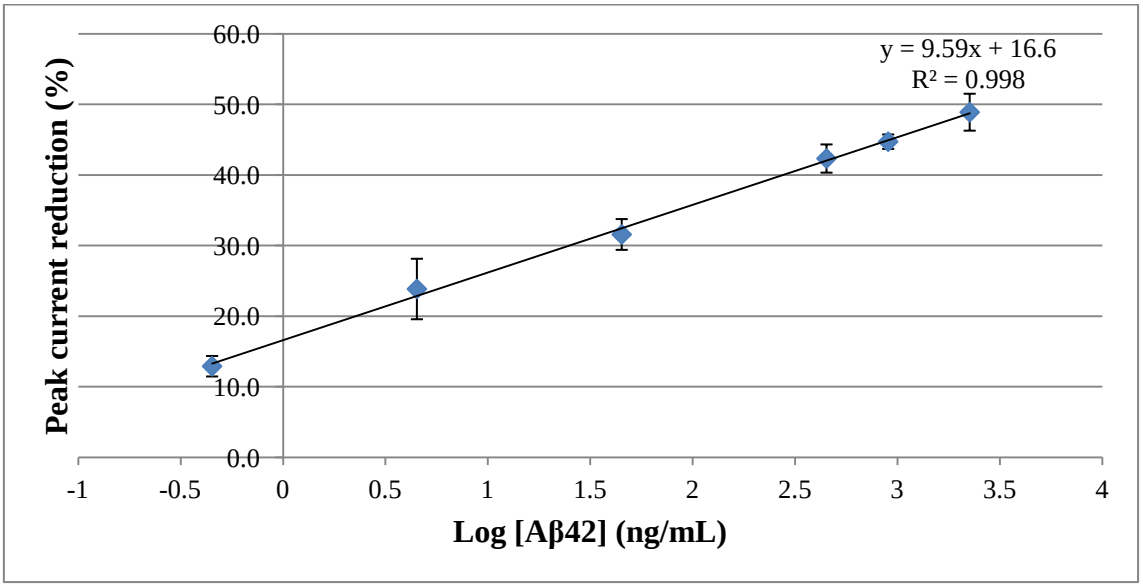

Figure 39 - Analytical curve of Aβ42 obtained with the developed immunosensor. Error bars correspond to two replicates.

The accuracy of the proposed biosensor was tested by recovery assays performed at two spiking levels. Recoveries of 94.6% and 96.6% were reached at the

fortification concentration of 903 and 451 ng/mL, respectively. The high sensitivity of the immunosensor can be attributed to the combination of the high performance of the gold electrode, versatility of the AuNPs and high affinity of the antibody-antigen binding. The detection of low levels of Aβ42 is fundamental for the early detection and monitorization of Alzheimer's disease. In addition it also enables the determination of high levels of Aβ42 which is important for advanced cases of Alzheimer's disease since the AD diagnostic is mainly performed by exclusion of other diseases.

5. Conclusion and Future directions

In this work, an electrochemical immunosensor for Alzheimer's disease Aβ42 biomarker is presented. The immunosensor construction started with the testing of different self-assembled monolayers on the gold electrode surface. This is a simple technique to modify the surface of materials and to control the interface between the electrode and the solution. The mercaptopropionic acid SAM formation, promoted a large signal reduction caused by the strong adsorption of the mercaptopropionic acid on the gold surface hampering the electron transfer process between the electrode surface and the solution. Cystamine and mercaptopropionic acid + mercaptoethanol had similar results.

Due to its excellent conductivity and catalytic properties, gold nanoparticles can act as an "electronic wire" and promote the communication between the redox centers in proteins and electrode surface. The catalytic activity of gold nanoparticles to amplify the electrochemical reactions gives them a significant priority in the design of electrochemical biosensors. AuNPs were electrodeposited on the SAM modified surface electrode and the electrical conductivity was reestablished causing a large signal enhancement. The next step was to immobilize the antibodies on the AuNPs. For that purpose, the antibodies were functionalized to promote immobilization with proper orientation. The quantification of Aβ42 was based on the percentage of current reduction of the redox pair $Fe(CN)_6^{3-/4-}$ caused by the specific interactions between the antibody and Aβ42. This label free technique exhibited analytical relevance in a wide concentration range (0.451 to 2257 ng/mL), with a detection limit of 264 pg/mL. The immunosensor accuracy was preliminary attained by recovery tests.

The developed biosensor offers interesting possibilities for detection of the selected biomarker since it uses simple and relatively inexpensive instrumentation. Its application is intended to be cheaper, easier and faster than conventional methodologies while being amenable to integration for *in situ* determination. It constitutes a novel approach in AD clinical diagnosis and theragnostics because biomarker levels are significantly related with stage of Alzheimer's disease.

In future studies the repeatability and reproducibility, as well as, the stability and possibility of regeneration of the immunosensor should be fully characterized. In addition, the developed immunosensor should be tested in real samples. However before performing these experiments the BSA immobilization is going to be implemented in

order to avoid nonspecific interactions that may occur between the immunosensor and interfering species present in fluid samples. Also, the possibility of using a second labeled antibody should be tested in order to increase the sensitivity and reduce the limit of detection.

Finally, characterization of the biosensor surface by scanning electron microscopy (SEM), transmission electron microscopy (TEM) and atomic force microscopy (AFM) should be performed to further confirm the SWV and EIS data.

6. References

1. Cummings, J.L. and G. Cole, *Alzheimer disease.* JAMA, 2002. **287**(18): p. 2335-8.
2. Alzheimer Portugal, *Doença de Alzheimer*. www.alzheimerportugal.org 2012 [cited 2012 5/6/2012].
3. Cummings, J.L., *Biomarkers in Alzheimer's disease drug development.* Alzheimers Dement, 2011. **7**(3): p. e13-44.
4. Hampel, H., et al., *Biological markers of amyloid beta-related mechanisms in Alzheimer's disease.* Exp Neurol, 2010. **223**(2): p. 334-46.
5. Andreasen, N. and K. Blennow, *Beta-amyloid (Abeta) protein in cerebrospinal fluid as a biomarker for Alzheimer's disease.* Peptides, 2002. **23**(7): p. 1205-14.
6. Hardy, J. and D.J. Selkoe, *The amyloid hypothesis of Alzheimer's disease: progress and problems on the road to therapeutics.* Science, 2002. **297**(5580): p. 353-6.
7. Gizeli, E. and C.R. Lowe, *Immunosensors.* Current Opinion in Biotechnology, 1996. **7**(1): p. 66-71.
8. Ju, H., X. Zhang, and J. Wang, *NanoBiosensing: Principles, Development and Application*. 2011: Springer New York.
9. Wijayawardhana, C.A., H.B. Halsall, and W.R. Heineman, *Electrochemical Immunoassay*, in *Encyclopedia of Electrochemistry*. 2007, Wiley-VCH Verlag GmbH & Co. KGaA.
10. Ronkainen-Matsuno, N.J., et al., *Electrochemical immunoassay moving into the fast lane.* TrAC Trends in Analytical Chemistry, 2002. **21**(4): p. 213-225.
11. Bard, A.J. and L.R. Faulkner, *Electrochemical Methods: Fundamentals and Applications*. 2000: Wiley.
12. Zoski, C.G., *Handbook of Electrochemistry*. 2007: ELSEVIER SCIENCE & TECHNOLOGY.
13. Pohanka, M. and P. Skladai, *Electrochemical biosensors - principles and applications.* Journal of Applied Biomedicine, 2008. **6**(2): p. 57-64.
14. Karran, E., M. Mercken, and B. De Strooper, *The amyloid cascade hypothesis for Alzheimer's disease: an appraisal for the development of therapeutics.* Nat Rev Drug Discov, 2011. **10**(9): p. 698-712.
15. Dickerson, B.C. and R.A. Sperling, *Neuroimaging biomarkers for clinical trials of disease-modifying therapies in Alzheimer's disease.* NeuroRx, 2005. **2**(2): p. 348-60.
16. Mahley, R.W., K.H. Weisgraber, and Y. Huang, *Apolipoprotein E4: a causative factor and therapeutic target in neuropathology, including Alzheimer's disease.* Proc Natl Acad Sci U S A, 2006. **103**(15): p. 5644-51.
17. Cedazo-Minguez, A., *Apolipoprotein E and Alzheimer's disease: molecular mechanisms and therapeutic opportunities.* J Cell Mol Med, 2007. **11**(6): p. 1227-38.
18. Harold, D., et al., *Genome-wide association study identifies variants at CLU and PICALM associated with Alzheimer's disease.* Nat Genet, 2009. **41**(10): p. 1088-93.
19. Lambert, J.C., et al., *Genome-wide association study identifies variants at CLU and CR1 associated with Alzheimer's disease.* Nat Genet, 2009. **41**(10): p. 1094-9.
20. Andersen, O.M., et al., *Neuronal sorting protein-related receptor sorLA/LR11 regulates processing of the amyloid precursor protein.* Proc Natl Acad Sci U S A, 2005. **102**(38): p. 13461-6.
21. Buongiorno, M., Y. Compta, and M.J. Marti, *Amyloid-beta and tau biomarkers in Parkinson's disease-dementia.* J Neurol Sci, 2011. **310**(1-2): p. 25-30.
22. Zetterberg, H., K. Blennow, and E. Hanse, *Amyloid β and APP as biomarkers for Alzheimer's disease.* Experimental Gerontology, 2010. **45**(1): p. 23-29.
23. Brett, C.M.A. and A.M.O. Brett, *Electrochemistry: Principles, Methods, and Applications*. 1993: Oxford University Press, Incorporated.
24. Gupta, V.K., et al., *Voltammetric techniques for the assay of pharmaceuticals—A review.* Analytical Biochemistry, 2011. **408**(2): p. 179-196.
25. Wang, J., *Analytical Electrochemistry*. 2006: Wiley.

26. Settle, F.A., *Handbook of instrumental techniques for analytical chemistry*. 1997: Prentice Hall PTR.
27. Koryta, J., J. Dvořák, and L. Kavan, *Principles of electrochemistry*. 1993: Wiley.
28. Kissinger, P.T. and W.R. Heineman, *Cyclic voltammetry.* Journal of Chemical Education, 1983. **60**(9): p. 702.
29. Chang, B.-Y. and S.-M. Park, *Electrochemical Impedance Spectroscopy.* Annual Review of Analytical Chemistry, 2010. **3**(1): p. 207-229.
30. Cornelis, R., et al., *Handbook of Elemental Speciation: Techniques and Methodology*. 2004: Wiley.
31. Li, Q., et al., *Miniaturized Electrochemical Immunosensor for Label-Free Detection of Growth Hormone.* Electroanalysis, 2012. **24**(6): p. 1272-1276.
32. Souza, D.d., S.A.S. Machado, and L.A. Avaca, *Voltametria de onda quadrada. Primeira parte: aspectos teóricos.* Química Nova, 2003. **26**: p. 81-89.
33. Souza, D.d., et al., *Voltametria de onda quadrada. Segunda parte: aplicações.* Química Nova, 2004. **27**: p. 790-797.
34. Lasia, A., *Electrochemical Impedance Spectroscopy and its Applications*, in *Modern Aspects of Electrochemistry*, B.E. Conway, J.O.M. Bockris, and R. White, Editors. 2002, Springer US. p. 143-248.
35. Grieshaber, D., et al., *Electrochemical Biosensors - Sensor Principles and Architectures.* Sensors, 2008. **8**(3): p. 1400-1458.
36. Yu, D., et al., *Biosensors in Drug Discovery and Drug Analysis.* Analytical Letters, 2005. **38**(11): p. 1687-1701.
37. Farré, M., et al., *Biosensors for Environmental Monitoring at Global Scale and the EU Level*, in *Biosensors for Environmental Monitoring of Aquatic Systems*, D. Barceló and P.-D. Hansen, Editors. 2009, Springer Berlin Heidelberg. p. 1-32.
38. Valdés, M., et al., *Analytical nanotechnology for food analysis.* Microchimica Acta, 2009. **166**(1-2): p. 1-19.
39. Barroso, M.F., et al., *Towards a reliable technology for antioxidant capacity and oxidative damage evaluation: electrochemical (bio)sensors.* Biosens Bioelectron, 2011. **30**(1): p. 1-12.
40. Viswanathan, S., et al., *Molecular imprinted nanoelectrodes for ultra sensitive detection of ovarian cancer marker.* Biosensors and Bioelectronics, 2012. **33**(1): p. 179-183.
41. Farré, M., et al., *Sensors and biosensors in support of EU Directives.* TrAC Trends in Analytical Chemistry, 2009. **28**(2): p. 170-185.
42. Liu, X., Q. Fan, and W. Huang, *DNA biosensors based on water-soluble conjugated polymers.* Biosens Bioelectron, 2011. **26**(5): p. 2154-64.
43. Wang, H., G. Shen, and R. Yu, *Chapter 9 - Aspects of recent development of immunosensors*, in *Electrochemical Sensors, Biosensors and their Biomedical Applications*. 2008, Academic Press: San Diego. p. 237-260.
44. Stefan, R.I., J.F. van Staden, and H.Y. Aboul-Enein, *Immunosensors in clinical analysis.* Fresenius Journal of Analytical Chemistry, 2000. **366**(6-7): p. 659-668.
45. Luppa, P.B., L.J. Sokoll, and D.W. Chan, *Immunosensors--principles and applications to clinical chemistry.* Clin Chim Acta, 2001. **314**(1-2): p. 1-26.
46. Pei, X., et al., *Sandwich-type immunosensors and immunoassays exploiting nanostructure labels: A review.* Anal Chim Acta, 2013. **758**: p. 1-18.
47. Viswanathan, S., C. Rani, and J.-a.A. Ho, *Electrochemical immunosensor for multiplexed detection of food-borne pathogens using nanocrystal bioconjugates and MWCNT screen-printed electrode.* Talanta, 2012. **94**(0): p. 315-319.
48. Fowler, J.M., et al., *Chapter 5 - Recent developments in electrochemical immunoassays and immunosensors*, in *Electrochemical Sensors, Biosensors and their Biomedical Applications*. 2008, Academic Press: San Diego. p. 115-143.
49. Killard, A.J., et al., *Antibodies: production, functions and applications in biosensors.* TrAC Trends in Analytical Chemistry, 1995. **14**(6): p. 257-266.
50. D'Orazio, P., *Biosensors in clinical chemistry-2011 update.* Clinica Chimica Acta, 2011. **412**(19-20): p. 1749-1761.

51. Mallat, E., et al., *Immunosensors for pesticide determination in natural waters.* Trac-Trends in Analytical Chemistry, 2001. **20**(3): p. 124-132.
52. Marco, M.-P., S. Gee, and B.D. Hammock, *Immunochemical techniques for environmental analysis I. Immunosensors.* TrAC Trends in Analytical Chemistry, 1995. **14**(7): p. 341-350.
53. Sadana, A. and T. Vo-Dinh, *Single- and dual-fractal analysis of hybridization binding kinetics: Biosensor applications.* Biotechnology Progress, 1998. **14**(5): p. 782-790.
54. Kong, T., et al., *CMOS-compatible, label-free silicon-nanowire biosensors to detect cardiac troponin I for acute myocardial infarction diagnosis.* Biosens Bioelectron, 2012. **34**(1): p. 267-72.
55. Lin, C.-C., et al., *Development of the multi-functionalized gold nanoparticles with electrochemical-based immunoassay for protein A detection.* Journal of Electroanalytical Chemistry, 2008. **619–620**(0): p. 39-45.
56. Neves, M.M.P.S., et al., *Voltammetric immunosensor for the diagnosis of celiac disease based on the quantification of anti-gliadin antibodies.* Sensors and Actuators B: Chemical, 2012. **163**(1): p. 253-259.
57. Viswanathan, S., et al., *Disposable electrochemical immunosensor for carcinoembryonic antigen using ferrocene liposomes and MWCNT screen-printed electrode.* Biosens Bioelectron, 2009. **24**(7): p. 1984-9.
58. Medyantseva, E.P., E.V. Khaldeeva, and G.K. Budnikov, *Immunosensors in Biology and Medicine: Analytical Capabilities, Problems, and Prospects.* Journal of Analytical Chemistry, 2001. **56**(10): p. 886-900.
59. Skládal, P., *Advances in electrochemical immunosensors.* Electroanalysis, 1997. **9**(10): p. 737-745.
60. Sadik, O.A. and J.M. Van Emon, *Applications of electrochemical immunosensors to environmental monitoring.* Biosens Bioelectron, 1996. **11**(8): p. i-xi.
61. Ghindilis, A.L., et al., *Immunosensors: electrochemical sensing and other engineering approaches.* Biosensors and Bioelectronics, 1998. **13**(1): p. 113-131.
62. Bange, A., H.B. Halsall, and W.R. Heineman, *Microfluidic immunosensor systems.* Biosens Bioelectron, 2005. **20**(12): p. 2488-503.
63. Delves, P.J., et al., *Roitt's Essential Immunology, Includes Desktop Edition*. 2011: Wiley.
64. Diaz-Gonzalez, M., et al., *Development of an immunosensor for the determination of rabbit IgG using streptavidin modified screen-printed carbon electrodes.* Talanta, 2005. **65**(2): p. 565-73.
65. Pemberton, R.M., T.T. Mottram, and J.P. Hart, *Development of a screen-printed carbon electrochemical immunosensor for picomolar concentrations of estradiol in human serum extracts.* J Biochem Biophys Methods, 2005. **63**(3): p. 201-12.
66. Aguilar, Z.P., W.R. Vandaveer, and I. Fritsch, *Self-contained microelectrochemical immunoassay for small volumes using mouse IgG as a model system.* Anal Chem, 2002. **74**(14): p. 3321-9.
67. Chemburu, S., E. Wilkins, and I. Abdel-Hamid, *Detection of pathogenic bacteria in food samples using highly-dispersed carbon particles.* Biosens Bioelectron, 2005. **21**(3): p. 491-9.
68. Rusling, J.F., *Nanomaterials-based electrochemical immunosensors for proteins.* The Chemical Record, 2012. **12**(1): p. 164-176.
69. Veetil, J.V. and K. Ye, *Development of immunosensors using carbon nanotubes.* Biotechnol Prog, 2007. **23**(3): p. 517-31.
70. Kim, S.N., J.F. Rusling, and F. Papadimitrakopoulos, *Carbon Nanotubes for Electronic and Electrochemical Detection of Biomolecules.* Adv Mater, 2007. **19**(20): p. 3214-3228.
71. Zacco, E., M.I. Pividori, and S. Alegret, *Electrochemical biosensing based on universal affinity biocomposite platforms.* Biosens Bioelectron, 2006. **21**(7): p. 1291-301.

72. Gitlin, G., E.A. Bayer, and M. Wilchek, *STUDIES ON THE BIOTIN-BINDING SITE OF AVIDIN - LYSINE RESIDUES INVOLVED IN THE ACTIVE-SITE.* Biochemical Journal, 1987. **242**(3): p. 923-926.
73. Jones, M.L. and G.P. Kurzban, *Noncooperativity of Biotin Binding to Tetrameric Streptavidin.* Biochemistry, 1995. **34**(37): p. 11750-11756.
74. Langone, J.J., *Protein A of Staphylococcus aureus and related immunoglobulin receptors produced by streptococci and pneumonococci.* Adv Immunol, 1982. **32**: p. 157-252.
75. Bjorck, L. and G. Kronvall, *Purification and some properties of streptococcal protein G, a novel IgG-binding reagent.* J Immunol, 1984. **133**(2): p. 969-74.
76. Akerstrom, B., et al., *Protein G: a powerful tool for binding and detection of monoclonal and polyclonal antibodies.* J Immunol, 1985. **135**(4): p. 2589-92.
77. Mohammad, F., *Specialty Polymers: Materials and Applications*. 2007: I.K. International Publishing House Pvt. Limited.
78. Ramanaviciene, A. and A. Ramanavicius, *Application of polypyrrole for the creation of immunosensors.* Critical Reviews in Analytical Chemistry, 2002. **32**(3): p. 245-252.
79. Korecka, L., et al., *Utilization of newly developed immobilized enzyme reactors for preparation and study of immunoglobulin G fragments.* Journal of Chromatography B-Analytical Technologies in the Biomedical and Life Sciences, 2004. **808**(1): p. 15-24.
80. Nelson, A.L., *Antibody fragments: hope and hype.* MAbs, 2010. **2**(1): p. 77-83.
81. Dong, S. and J. Li, *Self-assembled monolayers of thiols on gold electrodes for bioelectrochemistry and biosensors.* Bioelectrochemistry and Bioenergetics, 1997. **42**(1): p. 7-13.
82. Vericat, C., et al., *Self-assembled monolayers of thiols and dithiols on gold: new challenges for a well-known system.* Chemical Society Reviews, 2010. **39**(5): p. 1805-1834.
83. Timp, G., *Nanotechnology*, in *Nanotechnology*, G. Timp, Editor. 1999, Springer New York. p. 1-5.
84. Love, J.C., et al., *Self-Assembled Monolayers of Thiolates on Metals as a Form of Nanotechnology.* Chemical Reviews, 2005. **105**(4): p. 1103-1170.
85. Ulman, A., *Formation and Structure of Self-Assembled Monolayers.* Chem Rev, 1996. **96**(4): p. 1533-1554.
86. Gooding, J.J., et al., *Self-Assembled Monolayers into the 21st Century: Recent Advances and Applications.* Electroanalysis, 2003. **15**(2): p. 81-96.
87. Chaki, N.K. and K. Vijayamohanan, *Self-assembled monolayers as a tunable platform for biosensor applications.* Biosensors & Bioelectronics, 2002. **17**(1-2): p. 1-12.
88. Dubois, L.H. and R.G. Nuzzo, *Synthesis, Structure, and Properties of Model Organic Surfaces.* Annual Review of Physical Chemistry, 1992. **43**(1): p. 437-463.
89. Schilardi, P.L., et al., *Electrochemical deposition onto self-assembled monolayers: New insights into micro- and nanofabrication.* Chemistry-a European Journal, 2006. **12**(1): p. 38-49.
90. Whelan, C.M., et al., *Corrosion inhibition by self-assembled monolayers for enhanced wire bonding on Cu surfaces.* Microelectron. Eng., 2003. **70**(2-4): p. 551-557.
91. Daniel, M.C. and D. Astruc, *Gold nanoparticles: assembly, supramolecular chemistry, quantum-size-related properties, and applications toward biology, catalysis, and nanotechnology.* Chem Rev, 2004. **104**(1): p. 293-346.
92. Drechsler, U., B. Erdogan, and V.M. Rotello, *Nanoparticles: Scaffolds for Molecular Recognition.* Chemistry – A European Journal, 2004. **10**(22): p. 5570-5579.
93. Rogers, J.A. and R.G. Nuzzo, *Recent progress in soft lithography.* Materials Today, 2005. **8**(2): p. 50-56.
94. Venkataraman, L., et al., *Single-molecule circuits with well-defined molecular conductance.* Nano Lett, 2006. **6**(3): p. 458-62.
95. Newton, L., et al., *Self assembled monolayers (SAMs) on metallic surfaces (gold and graphene) for electronic applications.* Journal of Materials Chemistry C, 2013. **1**(3): p. 376-393.

96. Gates, B.D., et al., *New Approaches to Nanofabrication: Molding, Printing, and Other Techniques.* Chemical Reviews, 2005. **105**(4): p. 1171-1196.
97. Burshtain, D. and D. Mandler, *The effect of surface attachment on ligand binding: studying the association of Mg2+, Ca2+ and Sr2+ by 1-thioglycerol and 1,4-dithiothreitol monolayers.* Physical Chemistry Chemical Physics, 2006. **8**(1): p. 158-164.
98. Wang, J., *Nanomaterial-based electrochemical biosensors.* Analyst, 2005. **130**(4): p. 421-426.
99. Bučko, M., et al., *Immobilization in biotechnology and biorecognition: from macro- to nanoscale systems.* Chemical Papers, 2012. **66**(11): p. 983-998.
100. Luz, R.S., R. Iost, and F. Crespilho, *Nanomaterials for Biosensors and Implantable Biodevices*, in *Nanobioelectrochemistry*, F.N. Crespilho, Editor. 2013, Springer Berlin Heidelberg. p. 27-48.
101. Niemeyer, C.M., *Nanoparticles, Proteins, and Nucleic Acids: Biotechnology Meets Materials Science.* Angewandte Chemie International Edition, 2001. **40**(22): p. 4128-4158.
102. Katz, E. and I. Willner, *Integrated nanoparticle-biomolecule hybrid systems: synthesis, properties, and applications.* Angew Chem Int Ed Engl, 2004. **43**(45): p. 6042-108.
103. Fang, P.-P., et al., *Electrochemistry at gold nanoparticles deposited on dendrimers assemblies adsorbed onto gold and platinum surfaces.* Journal of Electroanalytical Chemistry, 2011. **659**(1): p. 76-82.
104. Vestergaard, M.d., et al., *Detection of Alzheimer's tau protein using localised surface plasmon resonance-based immunochip.* Talanta, 2008. **74**(4): p. 1038-1042.
105. Warner, M.G., et al., *Quantum dot immunoassays in renewable surface column and 96-well plate formats for the fluorescence detection of botulinum neurotoxin using high-affinity antibodies.* Biosens Bioelectron, 2009. **25**(1): p. 179-84.
106. Shan, Y., J.-J. Xu, and H.-Y. Chen, *Electrochemiluminescence quenching by CdTe quantum dots through energy scavenging for ultrasensitive detection of antigen.* Chemical Communications, 2010. **46**(28): p. 5079-5081.
107. Forzani, E.S., et al., *A Conducting Polymer Nanojunction Sensor for Glucose Detection.* Nano Letters, 2004. **4**(9): p. 1785-1788.
108. Ramanathan, K., et al., *Individually Addressable Conducting Polymer Nanowires Array.* Nano Letters, 2004. **4**(7): p. 1237-1239.
109. Kiselev, N.A., et al., *Carbon nanotubes from polyethylene precursors: Structure and structural changes caused by thermal and chemical treatment revealed by HREM.* Carbon, 1998. **36**(7-8): p. 1149-1157.
110. Viswanathan, S., et al., *Electrochemical immunosensor for cholera toxin using liposomes and poly(3,4-ethylenedioxythiophene)-coated carbon nanotubes.* Anal Chem, 2006. **78**(4): p. 1115-21.
111. Wang, J., *Nanoparticle-based electrochemical bioassays of proteins.* Electroanalysis, 2007. **19**(7-8): p. 769-776.
112. Sadik, O.A., A.O. Aluoch, and A. Zhou, *Status of biomolecular recognition using electrochemical techniques.* Biosens Bioelectron, 2009. **24**(9): p. 2749-65.
113. Dequaire, M., C. Degrand, and B. Limoges, *An electrochemical metalloimmunoassay based on a colloidal gold label.* Analytical Chemistry, 2000. **72**(22): p. 5521-5528.
114. Guo, S. and E. Wang, *Synthesis and electrochemical applications of gold nanoparticles.* Analytica Chimica Acta, 2007. **598**(2): p. 181-192.
115. Giljohann, D.A., et al., *Gold Nanoparticles for Biology and Medicine.* Angewandte Chemie-International Edition, 2010. **49**(19): p. 3280-3294.
116. Baptista, P., et al., *Gold nanoparticles for the development of clinical diagnosis methods.* Anal Bioanal Chem, 2008. **391**(3): p. 943-50.
117. Omidfar, K., F. Khorsand, and M. Darziani Azizi, *New analytical applications of gold nanoparticles as label in antibody based sensors.* Biosensors and Bioelectronics, 2013. **43**(0): p. 336-347.

118. Lu, F., et al., *Gold nanoparticles for diagnostic sensing and therapy*. Inorganica Chimica Acta, 2012. **393**(0): p. 142-153.
119. Ahirwal, G.K. and C.K. Mitra, *Gold nanoparticles based sandwich electrochemical immunosensor*. Biosens Bioelectron, 2010. **25**(9): p. 2016-20.
120. Turkevich, J., P.C. Stevenson, and J. Hillier, *A STUDY OF THE NUCLEATION AND GROWTH PROCESSES IN THE SYNTHESIS OF COLLOIDAL GOLD*. Discussions of the Faraday Society, 1951(11): p. 55-&.
121. Frens, G., *CONTROLLED NUCLEATION FOR REGULATION OF PARTICLE-SIZE IN MONODISPERSE GOLD SUSPENSIONS*. Nature-Physical Science, 1973. **241**(105): p. 20-22.
122. Kimling, J., et al., *Turkevich Method for Gold Nanoparticle Synthesis Revisited*. The Journal of Physical Chemistry B, 2006. **110**(32): p. 15700-15707.
123. Brust, M., et al., *SYNTHESIS OF THIOL-DERIVATIZED GOLD NANOPARTICLES IN A 2-PHASE LIQUID-LIQUID SYSTEM*. Journal of the Chemical Society-Chemical Communications, 1994(7): p. 801-802.
124. Jana, N.R., L. Gearheart, and C.J. Murphy, *Seed-mediated growth approach for shape-controlled synthesis of spheroidal and rod-like gold nanoparticles using a surfactant template*. Advanced Materials, 2001. **13**(18): p. 1389-1393.
125. Averitt, R.D., S.L. Westcott, and N.J. Halas, *Ultrafast electron dynamics in gold nanoshells*. Physical Review B, 1998. **58**(16): p. 10203-10206.
126. Xia, Y.N., et al., *Gold Nanocages: From Synthesis to Theranostic Applications*. Accounts of Chemical Research, 2011. **44**(10): p. 914-924.
127. Kim, F., et al., *Platonic gold nanocrystals*. Angewandte Chemie-International Edition, 2004. **43**(28): p. 3673-3677.
128. Doane, T.L. and C. Burda, *The unique role of nanoparticles in nanomedicine: imaging, drug delivery and therapy*. Chemical Society Reviews, 2012. **41**(7): p. 2885-2911.
129. Giljohann, D.A., et al., *Oligonucleotide loading determines cellular uptake of DNA-modified gold nanoparticles*. Nano Letters, 2007. **7**(12): p. 3818-3821.
130. Zhang, J.D. and M. Oyama, *A hydrogen peroxide sensor based on the peroxidase activity of hemoglobin immobilized on gold nanoparticles-modified ITO electrode*. Electrochimica Acta, 2004. **50**(1): p. 85-90.
131. El-Sayed, I.H., X.H. Huang, and M.A. El-Sayed, *Surface plasmon resonance scattering and absorption of anti-EGFR antibody conjugated gold nanoparticles in cancer diagnostics: Applications in oral cancer*. Nano Letters, 2005. **5**(5): p. 829-834.
132. Cheng, Y., et al., *Highly efficient drug delivery with gold nanoparticle vectors for in vivo photodynamic therapy of cancer*. Journal of the American Chemical Society, 2008. **130**(32): p. 10643-10647.
133. Kang, D.Y., et al., *Ultra-sensitive immunosensor for beta-amyloid (1-42) using scanning tunneling microscopy-based electrical detection*. Biosens Bioelectron, 2009. **24**(5): p. 1431-6.
134. Georganopoulou, D.G., et al., *Nanoparticle-based detection in cerebral spinal fluid of a soluble pathogenic biomarker for Alzheimer's disease*. Proc Natl Acad Sci U S A, 2005. **102**(7): p. 2273-6.
135. Tanaka, R., et al., *A novel enhancement assay for immunochromatographic test strips using gold nanoparticles*. Anal Bioanal Chem, 2006. **385**(8): p. 1414-20.
136. Miller, J.N. and J.C. Miller, *Statistics and Chemometrics for Analytical Chemistry*. 2005: Pearson/Prentice Hall.
137. Hamelin, A., *Cyclic voltammetry at gold single-crystal surfaces. Part 1. Behaviour at low-index faces*. Journal of Electroanalytical Chemistry, 1996. **407**(1–2): p. 1-11.
138. Granmayeh Rad, A., H. Abbasi, and M.H. Afzali, *Gold Nanoparticles: Synthesising, Characterizing and Reviewing Novel Application in Recent Years*. Physics Procedia, 2011. **22**(0): p. 203-208.
139. Link, S. and M.A. El-Sayed, *Size and Temperature Dependence of the Plasmon Absorption of Colloidal Gold Nanoparticles*. The Journal of Physical Chemistry B, 1999. **103**(21): p. 4212-4217.

140. Park, B.-W., D.-Y. Yoon, and D.-S. Kim, *Formation and modification of a binary self-assembled monolayer on a nano-structured gold electrode and its structural characterization by electrochemical impedance spectroscopy.* Journal of Electroanalytical Chemistry, 2011. **661**(2): p. 329-335.
141. Hermanson, G.T., *Bioconjugate Techniques*. 2010: Elsevier Science.
142. Vestergaard, M., et al., *A rapid label-free electrochemical detection and kinetic study of Alzheimer's amyloid beta aggregation.* Journal of the American Chemical Society, 2005. **127**(34): p. 11892-11893.
143. Prabhulkar, S., et al., *Microbiosensor for Alzheimer's disease diagnostics: detection of amyloid beta biomarkers.* J Neurochem, 2012. **122**(2): p. 374-81.
144. Li, H., et al., *Peptide-based electrochemical biosensor for amyloid β 1–42 soluble oligomer assay.* Talanta, 2012. **93**(0): p. 358-363.
145. Chikae, M., et al., *Amyloid-β detection with saccharide immobilized gold nanoparticle on carbon electrode.* Bioelectrochemistry, 2008. **74**(1): p. 118-123.